Future Foods 1–2 (2020) 100003

Contents lists available at ScienceDirect

Future Foods

journal homepage: www.elsevier.com/locate/fufo

Engineered food supplement excipients from bitter cassava for minimisation of cassava processing waste in environment

K.S. Tumwesigye[a,b], E. O'Brien[a], J.C. Oliveira[a], A. Crean[c], M.J. Sousa-Gallagher[a,*]

[a] Process and Chemical Engineering, School of Engineering, University College Cork, Food Science Building, Room308, College Road, Cork, Ireland
[b] National Agricultural Research Laboratories, NARO, Kawanda, Uganda
[c] School of Pharmacy, University College Cork, Ireland

ARTICLE INFO

Keywords:
Bitter cassava
Waste
SRRC-improved processing
Valorisation
Tablets
Iron-Zinc release

ABSTRACT

Unchecked large-scale rudimentary upstream (sub-merged and solid state) fermentation processes of bitter cassava roots into alcohol have often contributed significantly to agricultural wastes into environment. Thus, the study explored a proven valorisation methodology, Simultaneous Release Recovery Cyanogenesis (SRRC) along with intact bitter cassava polysaccharide-rich derivatives (CWF), as an apt to find alternative materials for food supplement excipients.

Triplicate CWF powder, peeled or intact bitter cassava roots, were produced and analysed to determine critical properties suitable in tablet making. Exclusion approach, using SRRC and compaction, was performed to select desired powder properties for tablet formulation. Microcrystalline cellulose, with known properties for developing drug excipients, was used as a validation reference material. Tablets, for disintegration time and in-vitro dissolution rates studies were produced using wet-granulation, and their potential to release and bio-avail Iron-Zinc investigated in-vitro (pHs 1.2 and 6.8 solutions, 37^0C). Morphology and Iron-Zinc dissolution-release mechanisms were examined. Kinetic models were used to describe matrix dissolution and Iron-Zinc release mechanisms.

Intact root powder compaction capacity, depicted by hardness, was 4.3, 4.4 and 4.6 KG at 200, 500 and 700 MPa respectively. Scanning Electron Microscopy (SEM) showed Iron-Zinc inclusion altered tablet morphology. Efficient matrix dissolution and Iron and Zinc release were achieved, showing apex recovery efficiency (98%, 30–45 min). Fitted models well-explained dissolution and release mechanisms (mean $R^2 = 0.95$), demonstrating adequacy.

SRRC-improved intact bitter cassava was confirmed as potential alternative excipient's matrix for Iron and Zinc release and bioavailability. Thus, this approach is practical for indirect waste elimination, and can promote strategy for sustainable valorisation of agricultural wastes and alternative functional food supplements delivery system.

1. Introduction

The increased utilisation of agricultural resources worldwide eventually has resulted into a higher generation of waste and by-products, causing serious environmental concerns and resource wastage (Ishangulyyev et al., 2019). It is estimated that over 30% (ca. 1.3 billion tonnes) edible food produced worldwide loses value (global economy loss of ca. $940 billion p.a) along the entire supply chain yearly (Abiad and Meho, 2018; FAO, 2020). This results in 793 million people undernourished and 870 million starved individuals (FAO, 2015), 8 percent of greenhouse gases (FAO, 2013). Worse still, waste management is posing unbearable challenge in developing countries caused by irreversible generation of wastes, underlying costs of disposal and defective handling systems (Abdel-Shafy and Mansour, 2018). The improving region-specific profiles of cassava as raw material for foods, feeds, pharmaceutical and confectionery industries have significantly accelerated unprecedented ventures into non-traditional underutilised food crops such as bitter cassava in the tropics (De Araújo et al., 2019; Mushumbusi et al., 2020; SahabUddin et al., 2015; Tumwesigye et al., 2016a). Roots of bitter cassava contain high levels of toxic total cyanide and free cyanide above 100 ppm fresh weight (fw) (De Araújo et al., 2019; McKey et al., 2010; Njankouo Ndam et al., 2019), with some tropical regions having bitter cassava with cyanide above 900 ppm fw (Manano et al., 2017). According to Schrenk et al. (2019), the minimum reference limit for cyanide is 0.02 mg/kg (ppm) dry weight (dw) body weight. Noteworthy, the peel (cortex) contains more cyanide than the edible portion (parenchyma). Most processing communities remove the peels being often discharged or underused, thus, representing great losses of feedstock and energy resources, as well as becoming po-

* Corresponding author.
E-mail address: m.desousagallagher@ucc.ie (M.J. Sousa-Gallagher).

https://doi.org/10.1016/j.fufo.2020.100003
Received 10 June 2020; Received in revised form 4 October 2020; Accepted 11 October 2020

tential sources of contamination, with negative environmental impact (Kemausuor et al., 2015; Malucelli et al., 2017). In some tropical regions, bitter cassava is transformed into alcohol using rudimentary fermentation processes. Unchecked large-scale rudimentary upstream and downstream process-fermentation of bitter cassava roots into food and alcohol have often contributed significantly to agricultural wastes into environment, leading to unsustainability. Valorisation of underutilised bitter cassava offers economic and environmental sustainability benefits by minimising residues, considered a major bottleneck to its full use (Torres-León et al., 2018). A promising alternative to transform bitter cassava wastes is the deployment of improved valorisation techniques. Waste valorisation (WV) is the idea of adding value to the waste stream in an economically viable manner (Lin et al., 2013). The WV popularity has attracted great attention in several applications such as packaging, pharmaceutical, nutraceutical (Galanakis, 2013), agro-chemical, polymer, biofuel manufacturing and functional foods among other industries (Fritsch et al., 2017; Varzakas et al., 2016).

Intact bitter cassava has the potential to provide sources of economically polysaccharide-rich derivatives (CWF) that could be used in the development of high value functional products (Silva et al., 2020). Previously, quality and safe CWFs were obtained from intact bitter cassava biomass using simultaneous release recovery cyanogenesis (SRRC) improved downstream processing methodology (Tumwesigye et al., 2016a). The SRRC was developed and optimised following the concept of waste valorisation (WV) and research on green materials from natural sources (Tumwesigye et al., 2016b). Completed research on valorisation of intact bitter cassava includes the SRRC of CWF polymers such as cellulose, holocellulose, lignin and other monosaccharides (Tumwesigye et al., 2016b) as well as the safety of CWFs, with acceptable levels of cyanide far away below the threshold limit (Tumwesigye et al., 2016a). The SRRC provides a rational process methodology for producing intact bitter cassava CWFs and limits the chance of producing solid wastes and reduces environmental effects (Tumwesigye et al., 2016a, 2016b, 2016c). The SRRC-produced CWFs have the advantage of a relatively low cost and rich derivatives compared with most of the commercial cassava starch (Tumwesigye et al., 2016a). Additionally, Alexis and Jean (2010) showed that CWFs of bitter cassava (cellulose, 41.6%; starch, 8.4% fw; carbohydrates, 94.70%) possess better properties than sweet cassava (cellulose, 2.95%; starch, 14.2% fw; carbohydrates, 94.62%). Moreover, evidence indicates that the CWF powder is a multifunctional and dynamic matrix (Tumwesigye et al., 2017; Versino et al., 2015) containing cellulose, hemicellulose, holocellulose as well as lignin (Tumwesigye et al., 2016b). Further, SRRC eliminates time and cost for additional drying, which in tropics resulted in aflatoxin contamination and made fermented cassava unsafe. The limit of 10 $\mu g/kg$ (ppb) including EU regulated limit of 2 $\mu g/kg$ for aflatoxin is recommended (Schrenk et al., 2019).

The above discoveries suggest that by evaluating properties of SRRC-produced CWF, the matrix suitable for application as excipients could be produced and used in the development of new oral tablet excipients for enhancement of bioavailability and stability of food supplements. Analytical data such as physical properties of CWF and derived tablets could be important factors for defining its application in excipient fabrication, and suitability as oral dosage forms for food supplements. For more than two decades, comprehensive research on suitable carrier and delivery systems has generated huge evidence demonstrating that biobased materials play a crucial function in drug and nutrient delivery and bioavailability outcomes (Martins et al., 2015). Research regarding excipients has systematically focused on conventional pharmaceutical carrier system involving oral dosage solid forms to enhance delivery and bioavailability (Dangre et al., 2016; Martínez-Ballesta et al., 2018). Although the oral administration route meant to ensure recipient satisfaction and compliance, has gained steadily, some orals may exhibit poor gastrointestinal instability and poor solubility as well as high cost (Censi and Di Martino, 2015; Khadka et al., 2014). Thus, pursuing a carrier and delivery process that is inexpensive, green and user-friendly is crucial to ensure a sustainable delivery system.

One common method in carrier and delivery systems is the development of excipients, which have the potential to enhance the bioavailability, stability and cost-effectiveness. Although, most tablet excipients have been used to deliver pharmaceutical drugs, the trend of their use in nutraceutical and supplements is fast growing worldwide (Choi et al., 2011; Firth et al., 2019; Moss et al., 2018; Oketch-rabah et al., 2020; Suleria et al., 2015). Current nutraceutical excipients' market growth trends are driven by changes in the consumer diet trends, influenced by high malnutrition incidences such as lack of micronutrients (Iron, zinc), and escalation of non-communicable diseases such as coronary heart

Nomenclature

B_d	bulk density
B_v	bulk volume
B_w	bulk weight
CI	complexibility/compatibility Index
C_e	initial concentration of Fe/Zn in excipient tablet matrix
C_s	initial amount of Fe/Zn in the solvent
Ct	micronutrient concentration in solvent at time, t
D_T	true density
D	deviation
d	diameter
E	dissolution efficiency
F	fracture force
F_t	function of time during micronutrient release from excipient
HR	Hausner ratio
h_w	hydrated residue weight
k	first order release coefficient
k_h	release constant of micronutrient from heterogeneous spherical tablet
k_o	erosion rate constant
k_s	constant stating structural characteristics of the excipient
l	overall length
$M_Ø$	total quality of Fe/Zn dissolved
M_t	quantity of Fe/Zn released in time t
$M_t/M_Ø$	fraction of Fe/Zn dissolved
M/M_o	cumulative fractional release of micronutrient from excipient
M_t, M_∞	Fe/Zn quantity released at time t and infinite time
n	release exponent describing release mechanism
P	porosity
ρ_{et}	tablet density
ρ_{tc}	true density of CWF_I
T_d	tapped density
TS	tensile strength
w	weight of tablets
$\hat{W}$	mean weight
w_d	residue dry weight
x	x-coordinate
X_o	initial radius of excipient tablet matrix
ϵ	tablet porosity
y	y-coordinate
π	ratio of table's circumference to its diameter
$\int_0^t y\,\delta x$	change in concentration of Fe/Zn at time t

diseases, obesity, diabetes and cancer. According to (Kaptoge et al., 2019), cardiovascular diseases caused death to 1.5 million people in 2012. Thus, increasing availability of nutraceutical excipients might be a solution to both iron deficiencies, non-communicable diseases and global pandemics (Galanakis, 2020). It is estimated that men iron requirement is on average 8.7 mg/ day, women who are menstruating need iron around 14.8 mg/day, and extremely iron-deficient groups may need up to 200 mg a day (Alleyne et al. 2008). Detailed adult requirements predict iron absorption of 16% in men and 18% in premenopausal women and children aged 12–17 years (EFSA, 2017). In infants aged 7–11 months, children aged 1–6 years, children aged 7–11 years, boys and girls aged 12–17 the requirement for absorbed iron is 0.79 mg/day require 5, 8, 8 mg/day EFSA, 2017). Males and females (7 months −25 years) require 7–11 mg/day and 5–8 mg/day Iron with corresponding Zinc requirements of 2.9–16.3 mg/day and 2.9–12.7 mg/day. Pregnant and lactating mothers (18–24 years) need 8.6 and 9.9 mg/day (Schrenk et al., 2019).

Nowadays, polymeric excipients have shown considerable potential in the delivery system as tablet binder, lubricant, anti-adhesives, tablet disintegrator, filling agent, coating agent, solubilising agent, stabiliser, emulsifying and gelling agents amongst other properties (Chatzizaharia and Hatziavramidis, 2015).

Nonetheless, it should be emphasized that the effect of SRRC on development CWF excipients and release and bioavailability of micronutrients iron and zinc has not been yet explored fully. Hence, the challenge for this study was to explore whether effective Iron and Zinc excipient manufacture and bioavailability might be influenced by SRRC-produced CWF. If low-cost tablets that are biocompatible with, and encapsulate adequately Iron and Zinc, as well as demonstrating necessary release can be achieved, then the CWFs could prove to be valuable platform materials to produce food supplement carriers. It is envisaged that this novel approach might open an innovative avenue to design excipient manufacture and food supplement delivery systems via the SRRC methodology.

Thus, the aim of this study was to: i) identify CWF with desired properties for making tablets; and (ii) determine disintegration time and simulate in-vitro dissolution, release rate and bioavailability.

To accomplish this task, the study was conducted into two stages (Fig. 1). In the first part, the experiment was intended to determine the sole effect of SRRC and intact bitter cassava on CWF properties that have potential in the development of new oral tablet excipients for enhancement of bioavailability and stability of supplements. Specifically, establish whether the novel CWF can be endowed with properties for the development of an ideal (self-sustaining) excipient with two or more functionalities such as good flowability and compressibility For the second part, the flowability and compression properties were optimised, based on the results obtained in the first stage, using granulation, and tablets were formulated with Iron and zinc and dissolution tested.

2. Materials and methods

2.1. Materials and reagents

Bitter cassava roots were obtained from producers' fields in northern Uganda. Different bitter cassava types are widely distributed in tropics and sub-tropics and are not fully utilised. Iron (II) sulphate heptahydrate (ACS reagent, ≥ 99%); and Zinc acetate (ACS reagent, ≥ 99%) were purchased from Sigma Aldrich Ireland. All the chemicals were used as they were without further modification or treatment, and in the form, they are available and absorbed in the body.

2.2. Cassava waste-based cellulosic fibre (CWF) biocomposite preparation

The CWF biocomposite employed in the excipient manufacture and bioavailability tests was recovered from the root biomass of intact bitter cassava (IBC) using SRRC improved downstream processing methodology (Tumwesigye et al., 2016a) without modifications. The IBC is well-described as comprised of whole root of cassava (Manihot esculenta Crantz), with its wastes (peel, cambium, phloem and central xylem fibre) and edible parenchyma as well as a renewable resource of minimal competition with food supply and a cost-effective option compared to the conventional use sweet cassava (Tumwesigye et al., 2016b, 2017). Using the SRRC methodology, two different samples, a treatment sample (labelled CWF_I) and a control (labelled CWF_P) were prepared. The CWF_I was obtained from intact root (without peeling) and CWF_P was extracted from the peeled root. The traditional methods of obtaining biomaterials includes peeling, and in this study, CWF_P was used as a control to determine the potential of using intact root, while exploring SRRC, on developing self-sustaining excipients. The composite powders of CWF_I and CWF_P used for subsequent tests were kept below 10% RH using a desiccator until analysed.

2.3. Validation of effectiveness of SRRC-produced CWF bio-composite powders

The performance of SRRC-produced CWF_I & CWF_P bio-composites were experimentally validated quantitatively using properties that have been proven to produce good quality tablets (Gabbott et al., 2016; Osamura et al., 2017). The aim was to establish whether the novel CWF can be endowed with properties for the development of an ideal (self-sustaining) excipient with two or more functionalities such as good flowability and compressibility. Thus, powder properties were evaluated.

2.3.1. Particle size and shape (PSS)

The PSS analysis was carried out by using woven wire test sieves in the 35 μm to 1 mm pore size range (Endecotts, UK), and by a Particle Size Analyser (CAMSIZER XT, Retsch Technology, Germany) with 1 μm - 3 mm pore size measuring range.

The sieves were stacked top-down according to sieve aperture in the 1.4, 90 and 710 μm range, a 50 g CWF_P bio-composites placed on the top sieve, and the sieving performed with auto-vibration for a fixed time of 10 min. This procedure was repeated for CWF_P bio-composites.

To ensure a uniform particle size, shape and distribution, the samples were further analysed using the CAMSIZER, and the results analysed by computer software (Quad Core PC, 8 processor).

2.3.2. Flow property analysis

The bulk density (B_d) and tapped density (T_d) were evaluated using a United States Pharmacopeia (USP) method (Manalo et al., 2018). A 10 g CWFs samples (moisture content, 1.6% w/w; ash content; 1.1% w/w; Iron, 0.03 mg/kg; zinc, 0.61 mg/kg; crude fibre, 1.09% w/w; crude lipid, 0.41% w/w) were transferred into a pre-weighed graduated cylinder (25 ml, 0.5 ml markings, 14.3 mm diameter). The bulk volume was recorded after manually tapping the cylinder 10 times on a flat tabletop surface. The tapped volume was recorded with the Electrolab ETD-1020 Tap Density Tester (Globe-Pharma, Toronto) after tapping raising the cylinder and allowing it to drop under a specified distance (WHO, 2019) in increments of 500 and 1250 taps with 250 drops per min. Triplicate tests were conducted for B_d and T_d.

The bulk density (B_d) was calculated as the fractional bulk weight (B_w) of the bulk volume (B_v) according to Eq. (1).

$$B_d = B_w / B_v \quad (1)$$

The B_w is the initial weight of the particles in the cylinder, and B_v is the initial volume before tapping (T).

The tapped density (T_d) was computed as the fractional bulk weight tapped density, expressed in Eq. (2).

$$Td = B_w / B_v \quad (2)$$

where, T_d, the tapped density.

A method (Cao et al., 2018) employing a gas pycnometer (AccuPyc II 1340; Micromeritics, Norcross, GA, USA) was used to measure the true density of the dried CWFs powder in triplicates.

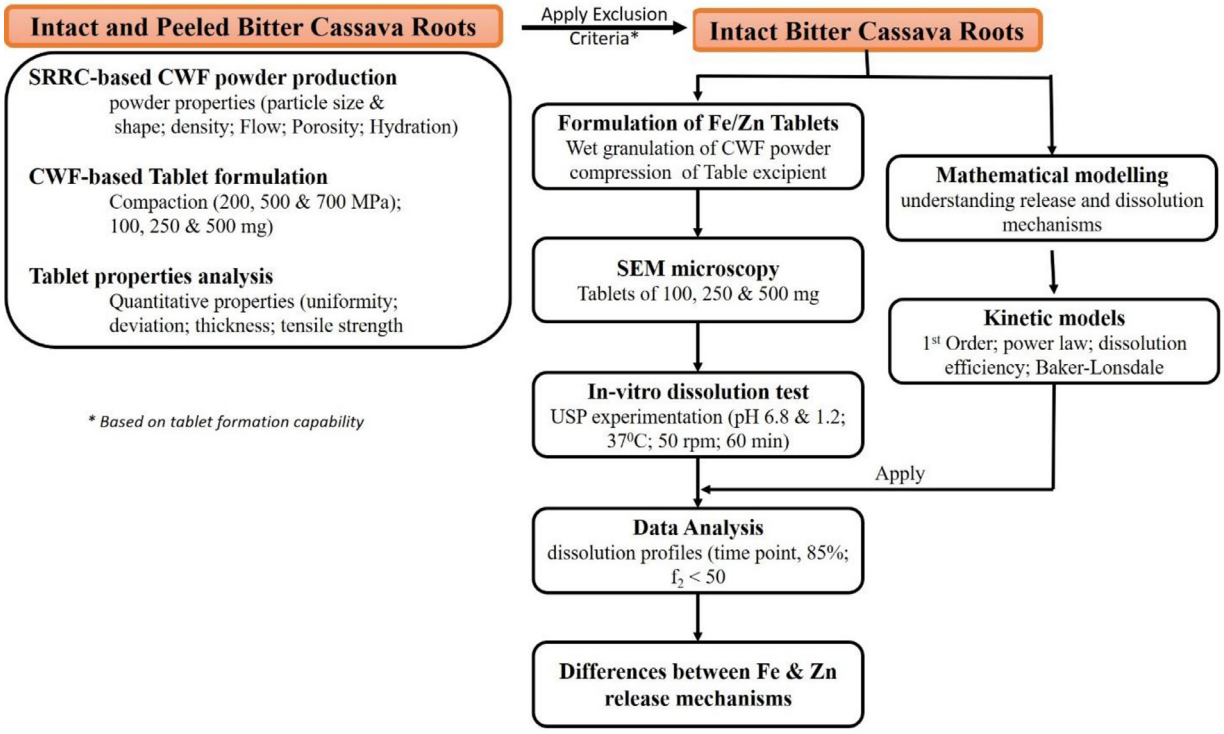

Fig. 1. Flow diagram depicting the methodological study of SRRC-produced CWF_I tablet.

The Carr's CI and HR provide insight into the flow properties and compressibility of powders (Shoaib et al., 2010). The CI was calculated from the B_d and T_d using Eq. (3), and the HR (Saifullah et al., 2014) computed by Eq. (4).

$$CI = \left[\frac{T_d - B_d}{T_d}\right]100 \tag{3}$$

$$HR = T_d/B_d \tag{4}$$

Determination of flow rate was achieved by introducing separately 40 g of CWF_P, CWF_I and MCC- Avicel PH-105 into a dry glass funnel of 10-mm orifice, and the time taken for the entire powder to flow out of the funnel was recorded. The procedure was replicated three times.

Angle of repose and angle of slide were measured by a powder integrative characteristic testing instrument (BT-1000, Bettersize Instruments Ltd., Liaoning, China) (He et al., 2018) without modifications. They are described as the maximum slant angle of the heap of powder against the plane without sliding down and the minimum slope angle for the flowing (He et al., 2018).

2.3.3. Porosity of CWFs

The CWF_P and CWF_I porosity was determined following the method (Hindi and Hindi, 2016) without modifications, Eq. (5).

$$P = \left[1 - \frac{B_d}{D_T}\right]100\% \tag{5}$$

where, B_d and D_T, bulk and true densities.

2.3.4. Hydration property (HP) analysis

The HP was based on water holding capacity (WHC), water retention capacity (WRC) and swelling capacity (SC) methods (Cao et al., 2018; Raghavendra et al., 2004) with slight modifications.

The WHC was determined by precisely weighing each of CWF_P, CWF_I and MCC powders (1 g) into graduated test tubes containing 30 mL of deionized water, and contents left to settle for 24 h. The supernatant was removed using a sintered glass crucible under vacuum, the hydrated residue weighed and dried at 90 °C until constant residual dry weight was achieved. The WHC was computed (Eq. (6))

$$WHC = \left[\frac{h_w - w_d}{w_d}\right] \tag{6}$$

where, h_w and w_d, hydrated residue weight (g) and residue dry weight (g).

To determine WRC, the procedure for analysing WHC was followed but in this case the contents were centrifuged (5000 g, 10 min).

The SC of CWF_P, CWF_I and MCC was done by precisely weighing dry powders (0.5 g) in a graduated test tube, and the initial volume recorded. After hydration in 30 mL deionised water for 24 h, the final volume was accurately measured. The SC was obtained by ratio of the volume occupied after hydration to the initial volume.

2.4. Preparation and analysis of tablet excipient from CWF bio-composites

Further to the quantitative measurement of CWF composites (Sections 2.3.1 and 2.3.2), a qualitative trial, involving the ability of both CWFs to form strong tablets was included in the performance evaluation. Following, a hydraulic hand press (Specac P/N 15,011/25,011, UK), set at different predetermined pressures (Table 2B) and constant volume (0.1 cc) was used to compact CWF into tablets (moisture content 1.5% w/w). Precisely, weighed CWFs samples were introduced into the press and compressed using stainless steel flat-circular punches (6.35 mm in diameter) with a constant force for pre-determined pressures, dwelling time of 5 t for 5 s at 20 °C and 30% relative humity).

To determine the effectiveness of intact bitter cassava based CWF to make quality excipients, a comparative study of known polymer material, microcrystalline cellulose, was run concurrently using the same procedure and test conditions.

The tablet quantitative properties were analysed as described hereunder.

The uniformity of weight of the tablets was determined by weighing, individually, a set of 20 tablets using a digital analytical balance (AXE 105 Delta Range ± 0.0001 g, Mettler-Toledo, Greifensee, Switzerland), and their weights averaged. The percentage deviation of the individual tablets from the mean was determined according to Eq. (7). No more than two of the individual masses should deviate from the average mass by more than the percentage deviation applicable for the tablet and, no individual mass should deviate by more than twice that percentage (Green et al., 2015; Patel and Patel, 2013; SahabUddin et al., 2015; Tumwesigye et al., 2016b).

$$D,\ \% = \left(\frac{\varpi - w}{\varpi}\right)100 \tag{7}$$

where, D, deviation; ϖ, mean weight; and w, weight of individual tablets.

Tablet thickness and diameter were measured by a Mitutoyo micrometre (Absolute Digimatic ID-S Série 543–790B; accuracy ± 0.003 mm, Codima Roboflux, Décines, France) immediately after compression as permitted by the (European et al., 2019) and reported in Juban et al. (2015) and (Tian et al. (2018).

Tablet tensile strength was determined two days after their formulation at 20 ± 5 ^{0}C by an ElectroPuls^{TM} E10000 Linear-Torsion All-Electric test instrument (Norwood, MA 02,062, USA). For each compression load (50 MPa, 100 MPa and 200 MPa), a minimum of six tablets per composition were tested, and the tensile strength (TS in MPa) was calculated according to (McKey et al., 2010) using Eq. (8).

$$TS = 2f/\pi l \tag{8}$$

where, f, fracture force; π, ratio of tablet's circumference to its diameter; d, diameter; and l, overall thickness.

Tablet Porosity was computed from the tablet density and true density of the CWF_I deploying Eq. (9).

$$e = \left[1 - \frac{\rho_{et}}{\rho_{tc}}\right] \tag{9}$$

where €, the porosity; ρ_{et}, tablet density; and ρ_{tc}, the true density of CWF_I.

Tablets disintegration times were measured according to the method described in (Vodáčková et al., 2018) with modification in number of tablets. Concisely, 10 tablets were disintegrated in deionised water at 37 °C using a ZT 301 (Erweka GmbH, Germany) apparatus.

The percentage friability of ten tablets was measured using a friabilator (Electrolab, India) according to (Mhase et al., 2018) without modification. Tablets were rotated at 25 rpm for 4 min (European et al., 2019). The tablets were then dedusted and the loss in weight caused by breakage or scratch recorded.

2.5. Experimental design, CWF_i bio-composite tablet preparation and Iron-Zinc dissolution process set-up

Following the failure of CWF_P to form real and hard tablets, they were discarded at this stage and only CWF_I bio-composite advanced for dissolution tests.

2.5.1. Design

The design inclusion of dissolution tests was defined based on three different tablet sizes, namely 100, 250 and 500 mg. The sizes were selected based on the common market sizes for pharmaceutical and nutraceutical excipients. A tablet excipient formulation design was used with four combinations (three treatments and blank) CWF_1, totalling twelve experimental runs in total (Table 1). The amount of Iron and zinc was incorporated in the tablets based on the design (Table 1) The quantities of Iron and zinc incorporated in the tablets were preferred based on the average recommended dietary requirements of men and women for maintaining their body mineral requirements (Anderson and Millen, 2017; "Dietary Reference Values for Nutrients Summary Report," 2017). It is widely known that the Iron and Zinc requirements are in the range of 8 mg/day for women and 11 mg/day for men (Roohani et al., 2013).

The principle of recipes is hinged on the requirement to have different quantities of Iron and zinc in the tablets based on the need to determine the effect of their concentration on release efficiency, and the need to have same total weight for all treatments. The latter reason is also true for the ratios selected.

2.5.2. Tablet

Granulation process: Tablet formulation was prepared initially by wet granulation of CWF_1 bio-composite powder using distilled water. Wet granulation is widely known to advance the properties of solid dosage formulations, mostly augmenting flowability, uniform weight, decreased segregation potential, reduced dusting, regulating residual moisture post-drying and improved compaction behaviour (Gabbott et al., 2016; World Health Organization, 2011). The CWF_1 powder (200 g) was loaded into a vessel and granulated using a 4M8 ForMate Granulator (Pro-CepT, Zelzate, Belgium). The powder was subjected to pre-mix conditions of 500 rpm impeller and chopper speeds for 3 min., and finally granulated using 1000 rpm impeller speed, 120% impeller torque, 2000 rpm chopper speed, 3 ml/min. dosing speed, 30 mL total dosing quantity, and 22 °C mixture temperature for 30 min. The granulated samples were dried in vacuum oven at 70 °C for 12 h. Moisture content was determined using PMX 60 Moisture analyser (Chromlab Scientific Services, UK), and a mean value of 2.25% was recorded. The dry granulated samples were sieved (Endecotts, UK) to diameter of 850 μm uniform particle size, and stored in a desiccator (20–22 °C; 0% RH) until further use.

Compaction process: Prior to compression, the contents of CWF_1 excipients, Iron (II) sulphate heptahydrate and zinc acetate (Table 1) were mixed uniformly in a low speed mixer (IKA Yellowline-R A 10, Germany) at 30 rpm for 30 min. A hydraulic hand press (Specac P/N 15,011/25,011, UK), set at 200 MPa was used to press the granulated samples into 100, 250 and 500 g tablets as described in subSection 2.3.3 (this study).

2.5.3. Scanning electron micrograph (SEM) tests

SEM images were taken under high vacuum on a Scanning Electron Microscope (SEM), JSM-5510 (Jeol Ltd., Tokyo, Japan) based on the method described (Tumwesigye et al., 2016b) with minimal modification. The accelerating voltage was 5.00 kV with a working distance of 15.0 mm. The sample was sputter coated with thin layer of gold using a vacuum evaporator.

2.6. Iron-Zinc disintegration and dissolution process set-up

2.6.1. In-vitro dissolution studies

In-vitro dissolution was determined simulating U.S. Pharmacopeia (USP) method as described (Cao et al., 2018; Psimadas et al., 2012; WHO, 2020) with modifications. The weighed excipient tablets (100, 250 or 500 mg) containing Iron (II) sulphate heptahydrate and zinc acetate were placed on a suspended mesh platform inside of a 300 mL beaker containing the 900 mL dissolution solvents at pH 1.2 achieved with 0.1 N hydrochloric acid (acid stage) (Fig. 1). The acid solution simulated gastric fluids (without enzymes) was initially equilibrated and maintained at 37 ± 0.5 °C (range of body temperature). A rotating paddle inserted in the beaker at a height of 25 mm from the tablet was used for stirring (50 rpm, 60 min.). To guarantee that the dissolution tests returned credible results, tablets with smooth, shiny and reasonably hard skin, with no visible defects, such as such as flecks, cracks, shape and size were sampled for the study. A sample was withdrawn after every 10 min and the undissolved excipients removed by filtration (Whatman no. 1 filter paper). An equal volume of the solution withdrawn for test

Table 1
Quantities of CWF_1 and various combinations with, Iron (Fe) and zinc (Zn) used in excipient development and dissolution studies; 100 mg (A); 250 mg (B) and 500 mg (C) tablet sizes.

	A Excipient Formulation (mg;%)							
	CWF_1	Portion,%	CWF_1+ Fe	Portion,%	CWF_1+Zn	Portion,%	CWF_1+ Fe +Zn	Portion,%
CS	100	*100*	50	*50*	75	*75*	25	*25*
FSH	0	*0*	50	*50*	0	*0*	50	*50*
ZA	0	*0*	0	*0*	25	*25*	25	*25*
TAS	100	*100*	100	*100*	100	*100*	100	*100*
	B Excipient Formulation (mg;%)							
	CWF_1	Portion,%	CWF_1+ Fe	Portion,%	CWF_1+Zn	Portion,%	CWF_1+ Fe +Zn	Portion,%
CS	250	*100*	200	*80*	225	*90*	175	*70*
FSH	0	*0*	50	*20*	0	*0*	50	*20*
ZA	0	*0*	0	*0*	25	*10*	25	*10*
TAS	250	*100*	250	*100*	250	*100*	250	*100*
	C Excipient Formulation (mg;%)							
	CWF_1	Portion,%	CWF_1+ Fe	Portion,%	CWF_1+Zn	Portion,%	CWF_1+ Fe +Zn	Portion,%
CS	500	*100*	450	*90*	475	*95*	425	*85*
FSH	0	*0*	50	*10*	0	*0*	50	*10*
ZA	0	*0*	0	*0*	25	*5*	25	*5*
TAS	500	*100*	500	*100*	500	*100*	500	*100*

CS, cassava waste; FSH, ferrous sulphate heptahydrate; ZA, zinc acetate.

was replaced. Immediately (within 5 min), a buffer dissolution solvent prepared by 0.2 M phosphate and equilibrated at 37 ± 0.5 °C was added to adjust pH to 6.8 (buffer stage). The procedure was continued, withdrawing sample after every 10 min until all the tablets were disintegrated.

Serial dilutions (1 mL) of the filtrate were made from 10 ml of the initial filtrate, and their UV absorbance recorded at 242 nm using a Biochrom Libra S22 UV/vis spectrophotometer (Cambridge CB4 0FJ, UK). A control containing only CWF_I excipient tablet was run concurrently. Similar quantities of Fe and Zn were dissolved in respective pH 6.8 and 1.2, serially diluted and used to derive standard curves. The experiment was replicated three times, and the data described quantitatively using mathematical models or used to illustrate dissolution profiles.

2.6.2. Application of mathematical models to explain Fe/Zn dissolution mechanism

Most excipients are developed in different forms and types resulting in different release mechanisms (slow, medium, fast), and this necessitates a dissection of the more elaborate models, in addition to kinetic model. This helps to understand the behaviour, type of release and angle of application of intact bitter cassava based CWF_I. Fe/Zn dissolution can be best interpreted by kinetic models, similar to what has been used in drug dissolution (Mužíková et al., 2018; Nirmala and Suresh, 2018). The model spells out the quantity (Q) of Fe/Zn dissolved as the function of dissolution time (t), i.e., Q = ƒ (t). Based on this background and the types of excipients developed in this study, and in addition to kinetics of release, the first order kinetics, power law, Baker-Lonsdale and Katzhenler and co-worker's models (Mužíková et al., 2018; Nirmala and Suresh, 2018) were applied for the interpretation of dissolution.

When the excipient is dissolved in the test solvent, it undergoes absorption which occurs, first, at the surface. This involves a single reactant-the Fe/Zn release, and thus the First order kinetic model (Gibaldi and Feldman, 1967; Phillips et al., 2012; Wagner, 1969), can be applied to describe the dissolution phenomena (Eq. (10))

$$\log C_t = \log C_s + \frac{kt}{2.303} \tag{10}$$

where, C_t, Fe/Zn concentration in solvent at time, t; C_0, initial amount of Fe/Zn in the solvent; and k, first order release coefficient.

This provides straight line graphs when the c-t graph is developed and gives the description of proportionality of Fe/Zn release.

In ideal situations, the diffusion and release of nutrients should follow the Fickian law. Nonetheless, due to differences in experiments, anomalous behaviour dominates solute motions. Thus, a more generic power law (Eq. (11)) suggested (Peppas et al., 2014) was used to study behavioural release of micronutrient from the novel intact bitter cassava CWF_I excipients.

$$F_t = k_s t^n \tag{11}$$

where, F_t, function of time that is represented by M_t / M_0, the cumulative fractional release of micronutrients from the excipient; k_s, constant defining the structural characteristics of the excipient; and n, release exponent describing the release mechanism. The general dependence of n on the diffusional mechanism is a function of excipient chemical composition and geometry (Caccavo et al., 2015). For a spherical geometry like the tablets in this study, the mechanism follows the assessment of solute diffusional release by Siepmann and Peppas (2012).

Application of (Baker, 2015; Fan Liang-tseng, 1989) was aimed at describing the micronutrient release from the heterogeneous spherical excipient tablets. It is important to note that most nutraceutical excipients are often heterogeneous, and this could have a significant influence on micronutrient release mechanism. Thus, to determine any possible loosening within the tablet matrix such as fissures or streaks, Baker-Lonsdale equation (Eq. (12)) was used:

$$F_t = \frac{3}{2}\left[1 - \left(1 - \frac{M_t}{M_\infty}\right)^{\frac{2}{3}}\right] - \frac{M_t}{M_\infty} = k_h t \tag{12}$$

where, M_t and M∞, Fe/Zn quantity released at time t and infinite time; and k_h, release constant (slope)

In perfect homogeneous excipients, the release of Fe/Zn would assume uniform surface erosion. However, due to anticipated heterogeneous erosion nature of current excipients, a model developed (Katzhendler et al., 1997; McConville et al., 2005) was explored (Eq. (13)).

$$\frac{M_t}{M_\phi} = 1 - \left[\frac{k_0 t}{C_e X_0}\right]^n \tag{13}$$

where M_t, quantity of Fe/Zn dissolved in time, t; M_ϕ, total quantity of Fe/Zn dissolved when the excipient tablet is fully exhausted; M_t/M_ϕ, fraction of Fe/Zn dissolved; k_0, erosion rate constant; C_e, initial concentration of Fe/Zn in excipient tablet matrix; X_0, initial radius of excipient tablet matrix; and $n = 3$ (for spheres). It was assumed that there was no influence of internal and external resistance perpendicular to the erosion.

Tablet excipient dissolution efficiency (E,%) was determined from the area under the curve of C-t plot of Iron/zinc dissolved at time, t or can be derived from Eq. (14) (Chatzizaharia and Hatziavramidis, 2015; Khan, 1975).

$$E,\ \% = \left(\frac{\int_0^t y\ \delta x}{y_{100}\ t}\right) * \ 100 \tag{14}$$

According to Pharmacopoeias, the acceptance dissolution limit is, $t_{45} \geq 80\%$.

2.7. Statistics

Statistical significance ($p \leq 0.05$) for the differences between the tensile strengths of the dispersed and agglomerated formulations was evaluated by ANOVA (α =5%). The Tukey test was used to show homogeneous powder and tablet parameters following post hoc test. Dissolution profiles were assessed by calculating the similarity factor f_2 according to the instructions of the (Food and Drug Administration, 2019). Only one time point after 85% of drug released was included in f_2-value calculations. Should the f_2-value be less than 50, the dissolution profiles were considered different (Diaz et al., 2016; Stevens et al., 2015).

3. Results and discussion

3.1. Identification of suitable CWF for enhancing tableting using exclusion approach

The improved downstream processing SRRC methodology allowed identification between CWF_I and CWF_P bio-composites with suitable properties for excipient tablet production (Fig. 1).

3.1.1. Quantitative evaluation of CWF

The effect of SRRC on particle distribution in different CWF samples compared to microcrystalline cellulose (MCC-Avicel PH-105) is presented in S-1 (supplementary data), showing that particle size and shape distribution of CWF_P and CWF_I followed the same pattern as that of MCC-Avicel PH-105, although MCC-Avicel PH-105 showed a slightly more uniform distribution when it was compared with the CWFs. Fabrication of tablet excipients has been shown to be a function of the uniformity of particle sizes in the starting formulations, which makes compaction more effective, and thus regulated delivery matrices (Alyami et al., 2017; Eyjolfsson, 2014).

It can be understood that while there was unevenness in distribution, which might be due to less quantity of CWFs used compared with MCC-Avicel PH-105, the distribution demonstrated the same pattern, signifying that within margin of error, CWF_I and MCC-Avicel PH-105 presented < 3 mm. The d-values define the diameters of the sphere which divides the samples weight into a specified percentage when the particles are arranged on an ascending mass basis (Grdešič et al., 2016). Thus, d_{50} and d_{90} describe the diameters at which 50% and 90% of the sample's weight comprised particles with a diameter less than the respective values. Accordingly, the d_{50} of CWF_I, CWF_P and MCC-Avicel PH-105 were in the region < 0.3, < 0.8 and < 1.0 mm, while their respective d_{90} were < 2.8, < 3 and < 4 mm. Evidently, 90% of CWF_I particle distribution was within < 3 mm.

To enrich the particle size and shape results and further determine the best tablet forming composite, the CWF_I and CWF_P were subjected to a more in-depth study using flow properties i.e. bulking Eq. (1)-(4),

Table 2
Physical properties of intact bitter cassava biomaterial (A) and tablets (B).

A

Parameter	Bulk density, g cm^{-3}	Tapped density, g cm^{-3}	True density, g cm^{-3}	Carr's Index,%	Hausner's Ratio	Flow rate, g s^{-1}	Angle of repose, ^{0}	Porosity,%
Cassava, CWF_P	0.61±0.0**a**	0.75±0.0**e**	1.57±0.1**i**	13.17±0.4**j**	1.23	10.13±1.0**n**	43.24±0.8**r**	74.78±1.2**v**
Cassava, CWF_I	0.38±0.0**b**	0.43±0.0**f**	1.49±0.2**i**	9.38±0.0**k**	1.13	20.91±0.8**p**	28.52±0.2**s**	68.87±0.9**w**
Microcrystalline cellulose, MCC	0.48±0.0**cd**	0.53±0.0**gh**	1.50±0.1**i**	8.35±0.0**lm**	1.10	19.94±0.2**pq**	41.20±0.6**tu**	75.78±1.1**vx**

B

Parameter	CWF_P	CWF_I	MCC	CWF_P	CWF_I	MCC	CWF_P	CWF_I	MCC	AC
CP, MPa	200	500	700							
Hardness, KG	*	4.32±0.8**a**	5.38±1.9**d**	*	4.42±0.1**b**	6.64±2.3**e**	2.34±4.4	4.64±1.0**c**	6.66±3.**57ef**	4–10
Diameter, mm	*	13.09±0.0g	12.96±0.0g	*	13.08±0.0g	12.95±0.0g	13.12±0.1	13.07±0.0g	12.96±0.07g	–
Thickness, mm	*	3.16±0.0**h**	3.19±0.1**h**	*	3.14±0.1**h**	3.04±0.1**i**	3.10±0.1	3.11±0.0**h**	3.05±0.08**i**	–
Weight, mg	*	546.36±2.8**j**	547.65±8.5**j**	*	551.48±9.0**k**	543.78±5.6**j**	552.58±11.5	542.62**j** ±4.7**j**	547.08 ±12**j**	544–648
TS, MPa	*	0.35±0.0**m**	8.3±0.3**p**	*	0.37±0.0**m**	10.86±1.1**q**	0.36±0.0	0.41±0.0**n**	10.75±1.3**q**	–
DT, s	*	903±2.3r	899±1.1r	*	895±1.3r	895±0.9**t**	1005±5.1	878±2.5s	861±1.3**u**	1800
Friability,%	*	0.67±0.1v	0.54±0.0**x**	*	0.56±0.0**w**	0.53±0.0**x**	0.85±0.1	0.51±0.0**w**	0.51±0.0**x**	nmt 1.00[a]

[*] Indicates failure of CWF_P to form tablets at pressures 200 and 500 MPa.

[a] Acceptance criteria based from the USP 40 Acetaminophen Tablets Monograph. Nmt – not more thanCP, compaction pressure; DT, disintegration time; TS, tensile strengthValues market with different letters vertically (A) and horizontally (B) are significantly different ($p \leq$).

flowability, porosity and hydration capacity (Table 2). Powder flow is a key criterion in production of solid dosage forms, mainly in the functionality of direct compression excipient, and as a function of tablet weight, hardness, and content uniformity (Achor et al., 2015).

The CWF_I bulking analysis showed that tapped, bulk and true densities are lower than those of CWF_P (Table 2A).

The disparities in the results might be due to the nature of their particle size and shape distribution, with CWF_I revealing a more uniform particle size, and increased inter-particle voids (He et al., 2018) than for the CWF_P (S-1). The higher tapped densities than for bulk densities for the three matrices could be reflected in the existence of higher contract surface area (He et al., 2018), and beneficial to tablet filling (Zhao et al., 2015). It was also suggested the above phenomenon could lead to higher solubility and dispersibility (Zhao et al., 2015). Bulk, tap and true densities of a material can be used to predict the flow properties and its compressibility, thereby providing durable solid excipients with the desired strength, porosity and dissolution characteristics (Silva et al., 2013). Further, bulk and tapped value closeness defines the best flowing properties of the powder (Silva et al., 2013). In this study, CWF_I true density was found to lie within the range reported for microcrystalline cellulose (MCC-Avicel PH-105) reported values (1.42 – 1.668 g/cm^3, and close to a true density of a perfect cellulose crystal (1.582 – 1.512 g/cm^3) (Sun, 2005). The associative true densities of CWF_I and MCC-Avicel PH-105 is reflected in their particle and shape distribution as shown in (S-1). By contrast, the higher CWF_P true density might be due to a more heterogeneous particle size and shape, deviating from that of CWF_I and MCC-Avicel PH-105. Moreover, the differences between CWF_I and CWF_P bulking properties might be a function of their production in the SRRC process and handling (treatment and storage).

The low Carr's Index (CI) and Hausner ratio (HR) of CWF_I than that of CWF_P (Table 2A) might imply that the inter-particulate and intra-particulate of CWF_I material interactions were significantly lower than those of CWF_P. This meant that CWF_I composite presented better easy-flowing ability compared with CWF_P, even though CWF_I exhibited higher CI and HR than MCC-Avicel PH-105. The generally accepted designated excellent, good, fair, passible, poor, very poor and very poor flow properties of a powder have been reported with CI of 1–10, 11–15, 16–20, 21–25, 26–31, 32–37, > 38, and their equivalent HR of 1.00–1.11, 1.12–1.18, 1.19–1.25, 1.26–1.34, 1.35–1.45, 1.46–1.59, >1 (Carr, 1965; Kumar and Nanda, 2018). In contrast, as per (Hausner, 1981), the HR of 1.18, 1.19–1.25, 1.3–1.5 and > 1.5 represents excellent, good, passable and very poor. CI is a measure of bridge strength and stability while HR is related to interparticulate friction (Jan et al., 2017; Shah et al., 2008). Thus, it can be concluded that CWF_I, within the limits of experimental error, had a better near free-flowing ability, and close to that of MCC-Avicel PH-105, which demonstrated excellent flowability. In contrast, CWF_P had fair flowability (Table 2A). Thus, CWF_I presented a fairly excellent flow character, and therefore suitable for advancement to tableting analysis.

Hence, particle size and shape-based exclusion analysis indicated good distinction ability of the CWF_I and CWF_P biocomposite powders. This is supported by failure of CWF_P to make solid tablets during compaction with a manual press, leading to visual particle disintegration when touched with hands.

As shown in Table 2A, CWF_I and MCC flow rates are higher than for CWF_P while the former's angle of repose and porosity are lower than for the latter, with CWF_P indicating near porosity to MCC. The lower CWF_I angle of repose might be explained by its lower particle size, and indication of uniformity, inseparable, and more flowability of CWF_I than for CWF_P.

The results are consistent with studies on wheat bran superfine and red rice powders (Chen et al., 2015; He et al., 2018; Xi et al., 2018).

According to USP (2017), an angle of repose of 25–30 ^{0}, 31–35 ^{0}, 36–40 ^{0}, 41–45 ^{0}, 46–55° and >56° signals excellent, good, fair, passable, poor and very poor flow properties respectively. Thus, CWF_I (28.52 ^{0}) exhibited excellent flow properties as compared to MCC (41.20 ^{0}) and CWF_P (43.24 ^{0}), which demonstrated passable flow property. Results imply that the inter-particular cohesion was strongest in CWF_I and weakest in CWF_P and MCC. Similar weak inter-particular cohesion was demonstrated in yellow *M. indica* and *A. heterophyllus* seed-based starch (Manalo et al., 2018). Poor flow could be caused also by strong inter-particle contact resulting into interlocking and perhaps creation of arches, cakes and ratholes.

As presented in Fig. 2, powders had a significant impact on hydration capacity. The CWF_P hydration properties differed significantly ($p \leq 0.05$) from those of both CWF_I and MCC while it was not significantly different ($p > 0.05$) between CWF_I and MCC (Fig. 2a). Notably, all powders demonstrated highly significant ($p \leq 0.05$) differences between WRC and rest of the hydration properties (Fig. 2a). It is worth noting that when time of hydration was considered, all powders exhibited different phenomena (Fig. 2b). Overall, CWF_I powder had distinctly lower WRC over time than WHC and SC of CWF_I and MCC, nonetheless, the gap narrowed as hydration time increased. Moreover, the CWF_I WRC increased with time as CWF_I WHC and SC and MCC WHC, WRC, SC decreased with time. Further analysis showed that there were no significant differences among the hydration pattern and trend as time increased for CWF_I and MCC.

The higher hydration capacity of CWF_I and MCC than that of CWF_P might be explained by their observed small particle sizes providing larger surface area and surface energy. It has been postulated that the said phenomena could lead to big vicissitudes in powder matrix structure and support the dispersibility and solubility of the powder, and thus significantly improve the hydratability (He et al., 2018). Markedly, the higher CWF_I and MCC SC than for CWF_P could be explained by physical structural changes and hydration properties of fibres (Zhu et al., 2014), but also to their hydrophilic nature, which allows maximum moisture uptake. The material SC offers an intimation of its disintegrating ability, an indication of potential of CWFI and MCC to producing better disintegrating excipients.

3.1.2. Qualitative and quantitative evaluations of tablets

After quantitative screening, CWF_P and CWF_I were subjected to tableting analysis Eq. (6) and ((7)). The qualitative and quantitative measurements monitor whether CWF_P or CWF_I can form tablets by physical compaction and in an attempt to identify which one demonstrates the most relevant tablet performance. Specifically, measurements of importance encompassing tablet weights and other physical analyses are depicted in Table 2B.

The results pointed to uniformity of tablet weight from both CWF_P and CWF_I with mean weights of 453 mg and 484 mg, and mean deviation of 1.56% and 0.68% respectively. The deviations for both tablet types were lower than the recommended limit of 5% (Schmid and Löbenberg, 2010). The slightly high deviation of CWF_P could be attributed to differences in the bulk densities and particle size distribution during compression. It is shown that physical property analysis of tablets compacted by different pressures, CWF_P yielded tablets at very high pressure only, while CWF_I produced tablets when subjected to all pressures (Table 2B). The crumbling of CWF_P at medium and high pressures was mainly due to the inability of particles to compact. This could be ascribed to inherent chemical composition of the root. Intact-derived CWF_I had better properties due to its enriched chemical components compared to the peeled CWF_P derivatives, attributed to high concentrations of other polysaccharides mainly cellulose, hemicellulose, holocellulose, lignin, protein, reduced amylose content (Aripin et al., 2013; Leite et al., 2017; Tumwesigye et al., 2016b), possibly providing better particle cohesion, adhesion and less brittleness in the tablets. Moreover, earlier studies showed that bio-composites obtained with intact root derivatives had a better binding capacity and uniformity compared to starch-based derivatives, which characterised excluded CWF (Tumwesigye et al., 2016a), suggesting that it could be responsible for the observed pattern in tablet formation. In this study, the unique Tongolo variety was used at maturity age of 18 months. Its waste chemical composition was, in-

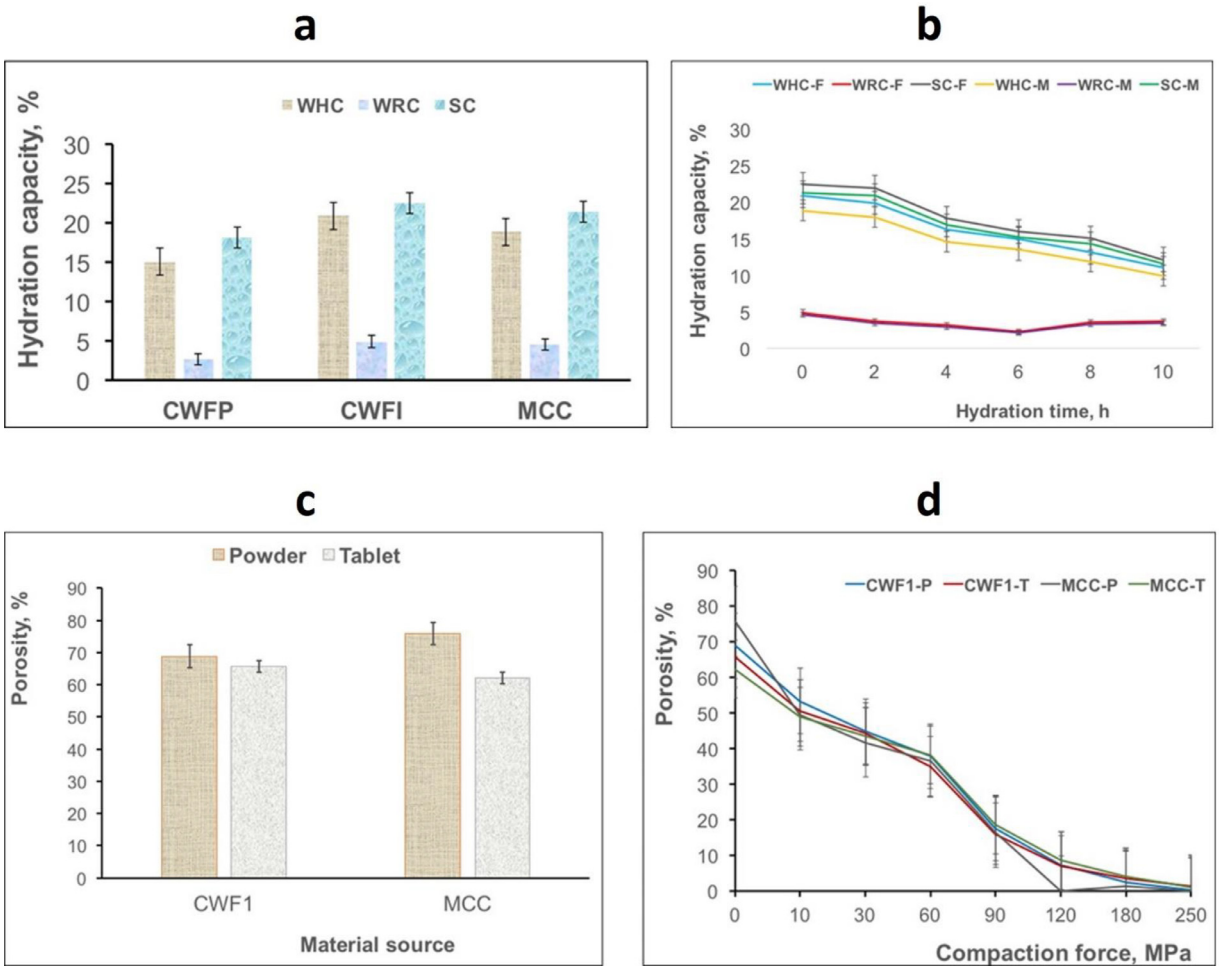

Fig. 2. Properties of biomaterials; hydration of CWF compared with MCC (a); impact of time on hydration capacity (b); Porosity of CWF tablet compared with powder (c); and effect of compression force on CWF powder and tablet porosity (d).

tact root CWF: cellulose (41.6%); lignin (13.4%); hemicellulose (25.5%); protein (6.2%); and starch (8.4%), and peeled root CWF: Cellulose 2.7%; lignin 1.1%; Protein 3.5% starch 14.2%. This was compared with sweet cassava, which included: cellulose (37.9%); lignin (23.9%); hemicellulose (7.5%); protein (5.3%); and starch (13.2%) (Aripin et al., 2013; Daud et al., 2013; Widiarto et al., 2019).

Further, this might be attributed to less uniform particle size and shape of CWF_P, which agrees with true, tapped and bulk densities obtained in this study (subSection 3.1.1). This could also be explained by CWF_P granule lower residual moisture content causing higher tablet porosity and increasing particle resistance to compression and reduces particle deformation (Gabbott et al., 2016; Nokhodchi, 2005). Uniformity of tablet weight and thickness are important parameters that indicate the amount of the active pharmaceutical ingredient present in the dosage form and ensure good packing of tablets (Ngwuluka et al., 2010). Thickness can vary without weight change due to difference in granulation density and pressure applied to tablets, as well as the speed of tablet compression (Chattoraj et al., 2018). Thus, as shown CWFI tablets exhibited reduced thickness as compression force increased in comparison to MCC.

To facilitate the interpretation of uniform weight phenomenon, physical analysis results are depicted in Table 2B. As shown in the table, both CWF_P and CWF_I tablets exhibited lower values of hardness and tensile strength than the MCC. This may be attributed to the nature of initial sample processing. MCC is universally produced by spray drying with the neutralized aqueous solution of strong acid hydrolysed cellulose slurry in order to manipulate the degree of agglomeration (particle size distribution) and moisture content (loss on drying) (Thoorens et al., 2014). By contrast, CWF_P and CWF_I is a product of weak acid hydrolysis that was oven dried. Unlike spray-drying, oven drying does not offer the desired agglomeration and controlled moisture loss (Maghsoodi and Yari, 2015). Thus, when CWF_P and CWF_I and MCC were subjected to direct compaction, MCC had improved compatibility or tabletability of the compression mix. Conversely, slightly higher CWF_I strength than that of CWF_P might be explained by the ability of the former granules to contain more residual moisture content after drying thus high plasticizing effect than the latter thereby reducing particle resistance to compression and enhancing particle deformation. Further, this might be due to lowered porosity at increased moisture content of CWF_I. Similar phenomenon has been reported elsewhere for powder and granules (Gabbott et al., 2016; Wade et al., 2013). A minimum of 4 KG crushing strength is required for satisfactory hardness. Slow release, oral and hypodermic and chewable tablets have 10–20, 4–10 and 3 KG crushing strength respectively (Vodáčková et al., 2018). The slightly lower but insignificant differences in crushing strength of CWF_P and CWF_I might be due to particle morphology of the initial materials as seen in this study. Thus, the desirable physical properties of intact bitter cassava CWF_P and CWF_I can be attained by improvements in the SRRC process, particularly with increased acid hydrolysis, and using a slightly older root (> 12 month maturity). Besides, the drying can be revisited to include spray drying (Murugesan and Orsat, 2012). Moreover, the results demonstrated that MCC can be applied as a strong binder, while CWF_P and CWF_I as poten-

tial weak binder and strong disintegrant (Kapoor et al., 2020). The latter property is supported by the dissolution rate results observed and can be central to the development of fast-release excipients (Sharma et al., 2019), mainly in instances where Fe and Zn are required in high adequate amounts and rapid availability (Roohani et al., 2013). Tablet hardness for all met the specification (Table 2B), with exhibiting higher values than CWFs in all compaction pressures. Tablet friability for CWFs showed comparable results with MCC and conformed to the criteria specified in the USP (Schmid and Löbenberg, 2010). These indicate that the produced tablets might be able to resist mechanical stress conditions in the distribution chain.

When the porosity of powder and tablet was compared, as expected powder matrix showed a higher value than the table matrix (Fig. 2c). Similarly, the effect of compaction force on tablet matrix porosity compared with the powder counter is presented in Fig. 2d, indicating a significant reduction in porosity as compaction force increases. Notably, except for MCC powder matrix at 120 MPa, tablet porosity demonstrated insignificant reduction pattern with powder porosity. According to Fig. 2d, the high porosity and resistance to compressibility of CWF_I-based tablet might be an indication of its powder containing particles of limited irregular shape with low variation in particle size, becoming more porous and failing to fill up void spaces between larger particles. The more porous CWF_I and MCC matrices indicate a reduced interparticular bond in the tablet, implying that the dissolution liquid could easily penetrate the tablets, which may result in a faster dissolution rate.

Further, the porosity pattern (Fig. 2d) might be attributed to the greater plasticity of the formulation matrix as indicated by low tensile strength (see Table 2B). The lower MCC porosity than CWF_I could be explained by the fact that smaller particle size allows flexibility for the tablets to pack more efficiently.

Disintegration times (DT) of tablets are presented in Table 2B, indicating an inverse proportion with compaction pressure. CWF_I exhibited higher DTs than MCC but not much difference was observed between two tablets; nonetheless, they conformed to USP (Schmid and Löbenberg, 2010) criteria. The DT is a measure of time required for the tablet to disintegrate into particles under a given set of conditions (Markl and Zeitler, 2017) and is reported to be influenced by the pore structure and bonding structure within the tablet. The higher CWF_I DT could be explained by a relatively higher CWF_I porosity and presence of large pores, which facilitated rapid water penetration into the tablet with a subsequent rupture of bonds, followed by disintegration of the tablet than MCC equivalent. It has also been proposed that the disintegrating medium may weaken the intermolecular bonds thus facilitating the disintegration of tablets as the efficacy of disintegrants is dependent on tablet porosity (Markl and Zeitler, 2017). The decrease in DTs could be explained by diminished tablet permeability with increased compaction time (Table 2B). The less effective DT of the excipients (lower DT than accepted criteria) could be attributed to relatively higher porosity causing swelling of excipient particles to exert less impact on the surrounding particles.

3.1.3. Comparison of physico-chemical properties of CWF_i with previous excipients

A comparison of different physico-chemical properties of previous excipients is presented (S-3, supplementary data), showing comparable flow properties and disintegration behaviour of current study excipients with previous excipients.

3.2. Evaluation of Fe-Zn excipient tablets

It is evident, from the preceding sections of this study and also widely accepted, that powder particulate nature, flow properties, pore structure and hydration capacity can regulate the tablet properties (e.g. tabletability, strength, disintegration) (Silva et al., 2013; Shah et al., 2008; Zhu et al., 2014). Thus, an understanding of the prior processing of the excipient before incorporation of Fe and zinc was necessary. However, since the purpose of the study was to assess the impact of intact bitter cassava and SRRC on the development of Fe and Zn excipients, only granulation was carried out on CWF_I powder. An example of excipient tablet prototypes with and without Fe and Zn produced from intact bitter cassava CWF_I, which were compared with that from peeled cassava are shown in Fig. 3.

3.2.1. Electron microscopy

To examine the impact of dispersion of Fe, Zn and Fe/Zn in tablet excipients on the homogeneity of the bio-derivatives, SEM was performed, and the results are presented in Fig. 4. A comparison of the SEM images revealed a less-heterogeneous morphology and microstructure of the matrices, non-aggregated and uniformly-blend matrices dispersed with Fe (Fig. 4ai), Zn (Fig. 4aii), Fe/Zn (Fig. 4aiii) than for the control (Fig. 4aiv). The similarities in the morphology and size of all matrices could be attributed to SRRC processing conditions and perhaps the less influence of dispersed Fe and Zn. The apparent tablet matrix near homogeneity lends a considerable dispersion of Fe and Zn, and waste bitter cassava derivatives as promising cellulosic fibre inert excipient tablets for oral dosage solid forms.

3.2.2. In-vitro nutrient release studies and mechanisms

In-vitro nutrient analysis: The combination of different weights of Fe and Zn in the formulation played a meaningful role in modifying the release behaviour of the CWF_I matrix tablet. The results of the release process of CWF_I–based excipient tablets are presented in S-2 (supplementary data), showing that dissolution time had a highly significant ($p \leq 0.05$) positive impact on Fe and Zn release, both linearly and quadratically. This result is expected and attributed to the fast release matrices (Kumar and Nanda, 2018; Morovati et al., 2017). Consistently, Zn had a preferential fast release to Fe as far as excipient weights, combined form and solution pH environment were taken into consideration. This could be attributed to the greater resistance to release of Fe from the matrix compared to Zn (Donangelo et al., 2002). Conversely, Zn might bond well with matrix particles thereby reducing porous structure, less hydration and slow release (Li and Mooney, 2016).

The release behaviours of CWF_I matrix tablets with different formulation of Fe-Zn were investigated by two pH-dependent dissolution media at pH 1.2 and 6.8 in order to mimic conditions of the Gastrointestinal tract. Following, the effect of using a single nutrient (Fe or Zn) and in different combining styles (Fe in Zn matrix; Zn in Fe matrix) on the release profiles of CWF_I matrix tablets was determined by transforming the dissolution data into profiles (Fig. 5).

The CWF_I-Fe (at pH 1.2), CWF_I-Zn (at pH 1.2), CWF_I-Fe/Zn (at pH 1.2 & 6.8) and CWF_I-Zn/Fe (at pH 1.2 & 6.8) dissolution profiles displayed two stages; firstly, the nutrient release corresponds to the nutrient transmission from the tablet surface. In the second stage, the residual nutrients release happens after the CWF_I matrix degradation. Observations for all profiles showed gradual increase in dissolution time involved hydration of the matrices, which became permeable and as a result the nutrients diffused slowly with time.

It can be noticed that for CWF_I/Fe; CWF_I/Zn; CWF_I/Fe in Zn; and CWF_I/Zn in Fe matrices, the cumulative release of Fe-Zn was in the range 50, 45, 25 and 25 mg in pH 1.2 and 22, 23, 40 and 42 mg in pH 6.8 media till 45 min, indicating that the matrices demonstrated slowest release rate in pH 6.8, and those with high weight. The slowest rates might be due to high intermolecular force interactions between Fe-Zn molecules and carrier matrices at high pH or high weight, producing a lower internal energy of nutrient-carrier than between Fe-Zn (Zhang et al., 2018). Further, it might be due to the uptake of water and swelling of CWF_I tablet containing Zn leading to faster disintegration and release Zn than Iron.

Nutrient release mechanism: To gain better understanding of the release nature of the excipient matrix, the dissolution data were fitted to different models Eqs. (8)–((12)), and the parameters are presented in Table 3. In all cases, the results correlate inversely with excipient mass,

Fig. 3. Excipient tablet prototypes used in in-vitro dissolution: a) from CWF_P; b) CWF_I; c) CWF_I with Fe and CWF_I with Zn; d) CWF_I with combined Fe and Zn; and e) MCC.

Table 3
Fitting of CWF release data to model equations.

Excipient system	Portion of nutrient in tablet,%	Solvent pH	Total mass dissolved	Rate constant, k 1st Order	Erosion	Loosening	Release exponent (n)	Dissolution efficiency,%	R^2
CWF_1/Iron	50	1.2	49.19 ± 0.05	0.017	1.121	0.183	0.865	96	0.922
	20		46.85 ± 0.04	0.016	0.455	0.172	0.866	92	0.913
	10		39.40 ± 0.44	0.029	0.285	0.227	0.889	76	0.948
		6.8	42.30 ± 0.06	0.110	0.914	0.482	1.271	80	0.866
			41.76 ± 0.31	0.111	0.958	0.478	1.273	78	0.864
			36.81 ± 0.12	0.136	1.810	0.434	1.064	70	0.932
CWF_1/Iron in Zinc matrix	25	1.2	44.58 ± 0.05	0.022	0.371	0.206	0.884	88	0.971
	10		43.90 ± 0.00	0.021	0.380	0.198	0.919	86	0.989
	5		36.88 ± 0.03	0.078	0.350	0.371	1.033	80	0.949
		6.8	42.80 ± 0.01	0.024	0.349	0.207	0.908	81	0.986
			42.43 ± 0.18	0.024	0.343	0.208	0.893	68	0.982
			34.99 ± 0.02	0.095	0.792	0.369	0.920	65	0.980
CWF_1/Zinc	25	1.2	24.87 ± 0.03	0.009	0.876	0.103	1.001	98	0.948
	10		24.93 ± 0.02	0.010	0.611	0.117	0.990	96	0.980
	5		24.21 ± 0.02	0.015	0.498	0.157	1.014	90	0.964
		6.8	22.49 ± 0.02	0.011	0.593	0.112	0.966	86	0.946
			22.29 ± 0.01	0.010	0.541	0.110	0.893	84	0.926
			20.20 ± 0.02	0.001	0.468	0.114	0.681	74	0.889
CWF_1/Zinc in Iron matrix	50	1.2	23.62 ± 0.02	0.017	0.449	0.169	1.015	94	0.941
	20		23.41 ± 0.02	0.018	0.372	0.177	0.988	92	0.960
	10		21.20 ± 0.01	0.018	0.379	0.160	1.009	84	0.946
		6.8	22.49 ± 0.05	0.022	0.303	0.208	0.898	90	0.971
			22.18 ± 0.02	0.021	0.454	0.203	0.929	89	0.964
			19.19 ± 0.01	0.112	0.623	0.212	0.888	76	0.950

and to a less extent when Fe and Zinc were combined in a single tablet regardless of the weight. This implies that the diffusion of the nutrients in the tablet matrix may be different (Lamoudi et al., 2016), despite the apparent similarities in hydration efficiency of solutions. In contrast, Fe and Zn were better released in acidic environment (pH 1.2) than the alkaline equivalent (pH 6.8), implying that they can easily be absorbed in the stomach. Taken together, Fe and Zn were highly released in solution medium as verified by their high dissolution efficiency.

The release exponent, n values demonstrate that the Fe-Zn dissolution from cassava CWF_I matrix was governed by polymer relaxation mechanism but not diffusion-controlled mechanism (Table 3), suggesting that the stress relaxation process is very slow relative to the rate of diffusion. This also demonstrates an anomalous behaviour in which the liquid diffusion and CWF_I relaxation rates exhibit similar magnitude. It is well-known that a desirable mechanism for any release process in various applications should provide zero-order release performance, with n falling around one ($n = 1$) (Hsu and Langer, 1985; Ritger and Peppas, 1987).

Apart from dissolution due to diffusion, the fast release rates observed in this study could be attributed to bitter cassava CWF_I excipient matrix erosion. As shown in Table 3, erosion rates (k_0) seem to be slightly higher compared to k_0 in drug dosage forms (Dürig et al., 1999) and elsewhere (Nep et al., 2015). Although erosion phenomena are exploited in drug dosage forms for the design of oral extended release, it might be of advantage when applied in micronutrient matrices designed specifically with heterogeneous surfaces for fast releases. In this study, surface heterogeneity seemed not to be the major contributor of erosion since the tablets produced showed fairly smooth surfaces (Fig. 4).

The high erosion rates might be also due to ability of cassava CWF_I to gel quickly, swelled and released the micronutrients as fast as it could. In this study, the slightly higher erosion values could be explained by the weak gel layer of the CWF tablet excipients (Efentakis and Buckton, 2002).

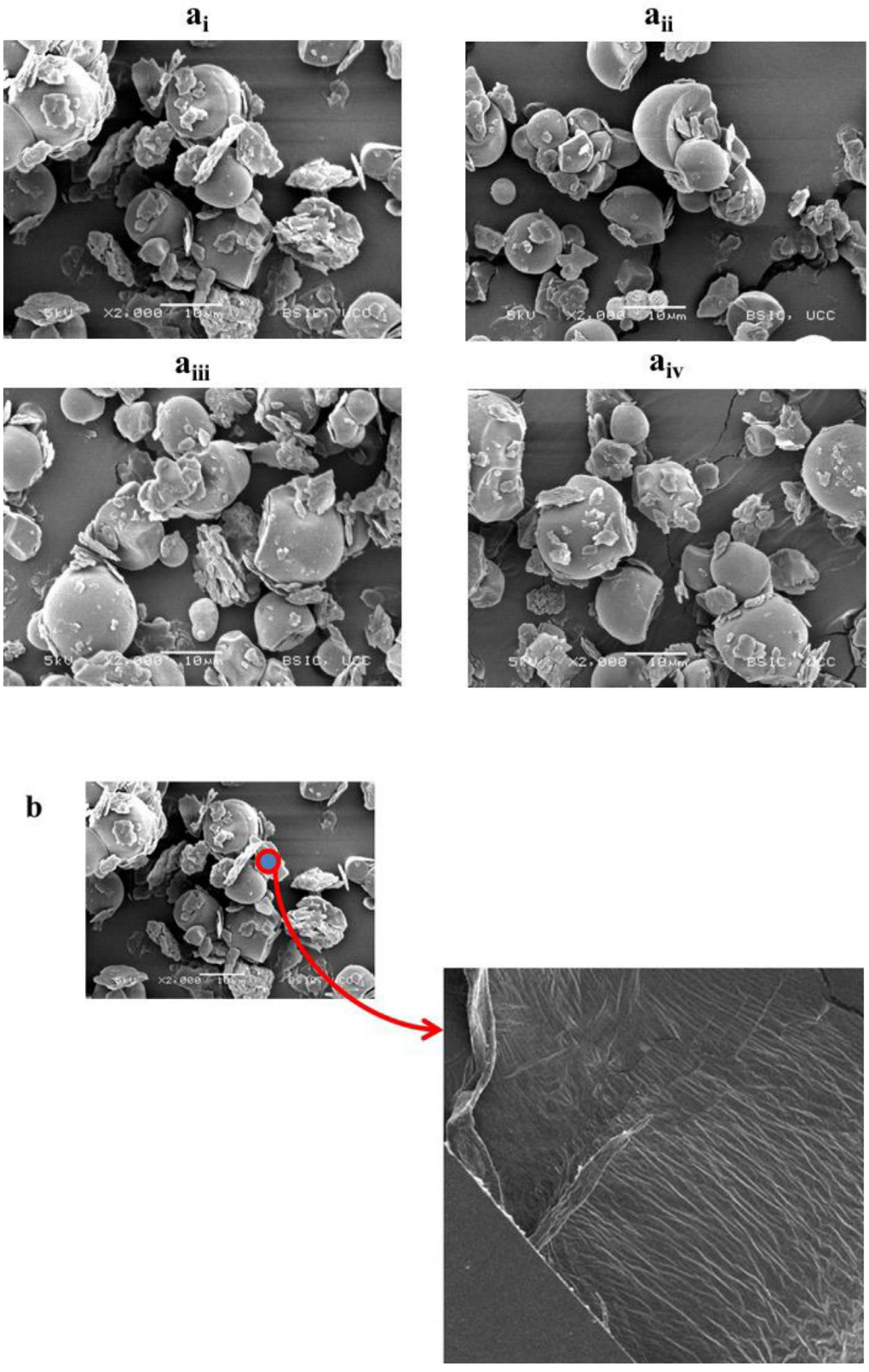

Fig. 4. SEM photographs of CWF_I tablet matrix: ai, aii, aiii) and aiv) after incorporation of Fe, Zn, combination of Fe and Zn and control; and b) showing fibres incorporated in the bio-derivatives during SRRC processing.

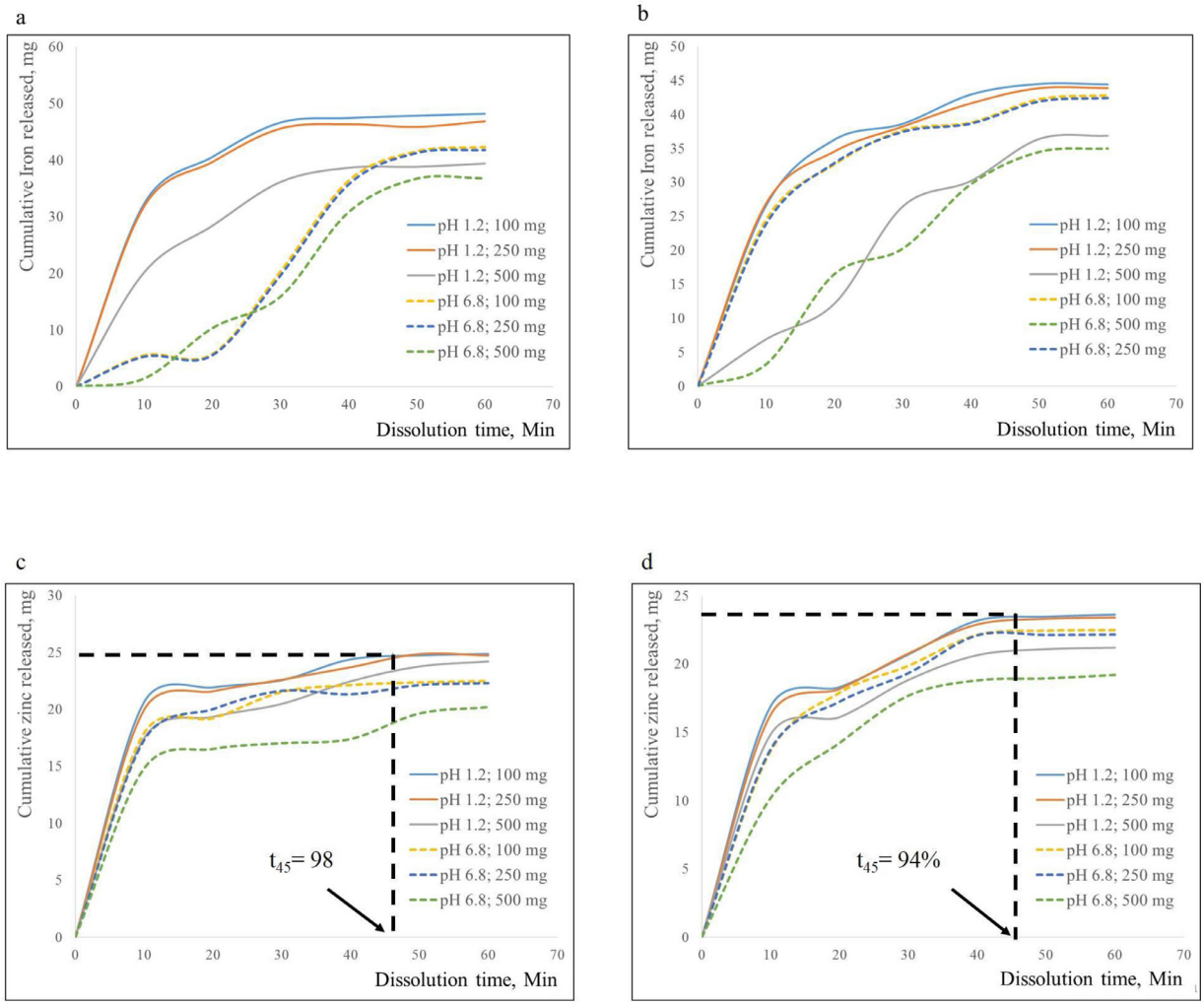

Fig. 5. Rate profiles of Fe/Zn release from CWF_I-tablet excipient: a) CWF_I/Fe (proportion of Fe 50, 20 &10%); b) CWF_I/Zn (proportion of Fe 25, 10 &5%); c) CWF_I/Fe in Zn (proportion of Fe 25, 10 &5%); and d) CWF_I/Zn (proportion of Fe 50, 20 &10%) in Fe matrices. Sample aliquots taken from the solution (and replaced with equal amounts) at specified intervals, and absorbance read.

While there seemed to be no visible heterogeneous surfaces, it seemed to indicate that heterogeneity could be localised within the internal parts of the tablet. As shown in Table 3, the slightly higher weight-dependence loosening with 500 mg than for 250 and 100 mg might suggest presence of porous, streaks or crevices with increased solids in the matrix. It might be expected that spaces within the matrix would lead to fast surface erosion by reducing solvent diffusion pathways. This was not likely with intact bitter cassava CWF_I since there is no correlation in the erosion and loosening constants (Table 3). This suggests that the fast releases could be a function of swelling of the tablet matrices or due to bulk erosion.

Additionally, in comparison to MCC-Avicel PH-105, it could be hypothesized that the powderier CWF_I, with less porous spaces would form thick gels inside its matrix and delay fast internal erosion. However, this was not possible with fast release rates observed.

The coefficient of determination, R^2 represents means for the entire model fitted. With mean R^2 values of 0.945, it showed a good fitting, which is an indication that they explain the Fe-Zn phenomena from intact bitter cassava CWF_I. It was noticed that dissolution efficiency for Fe and Zn was higher for pH 1.2 than in the pH 6.8, as shown by profile rates (Fig. 5). In particular, low-weight tablets demonstrated higher dissolution efficiency (DE) than for higher weight ones. The observed phenomena might be due to fast diffusion of the nutrients from the surface of the tablet matrix of low-weight tablets than for the higher-weight ones. The similar trend has been reported for drug release from tablet matrices (Lamoudi et al., 2016). Generally, the DE for pH 12-based matrices were within and above the acceptance dissolution limit is, $t_{45} \geq 80\%$ (Saccone et al., 2004). The Fe and Zn micronutrients were incorporated in the tablets in the form of sulphate and acetate, respectively, as they are presented in the body. Ionisation of these nutrients usually occurs when pH of the dissolution is lower (Sharp and Srai, 2007). This probably also explains the relatively higher release rates of Fe and Zn in intact bitter cassava CWF_I matrices in solvent at pH 1.2 in contrast to pH 6.8.

Generally, it is known that the mechanism of active ingredient release from excipients containing swellable polymers is multifaceted, with some systems categorized as either purely diffusion or erosion controlled, while most systems exhibit a combination of the two mechanisms (Glaessl et al., 2010; Lamoudi et al., 2016). As demonstrated in Table 3, the nutrient release, in pH 1.2 solution, from 100 to 250 g formulations of matrix tablets showed a good fit into Katzhendler and Baker-Lonsdale equations, indicating joint effect of loosening and erosion mechanisms for nutrient release. The release data fit well with the two models as a coefficient of determination (R^2) > 0.90 was obtained for all combinations. In pH 6.8 medium, the constant k was found to fluctuate feebly and with $R^2 < 0.90$, thus describing 1st order diffusional release of nutrients from the tablet.

Conclusion

Engineering of dietary supplement excipients for fast delivery of micronutrients, iron and zinc using intact bitter cassava polysaccharide-rich derivatives (CWF) and SRRC, is achievable.

The intact root based CWF_I is a better matrix with superior tableting properties and endowed with properties capable of producing excipients for fast delivery systems for Fe and Zn in acidic and neutral pH than one obtained from peeled based CWF_P. This provides hope of valorising circa 300 kg per ton of bitter cassava waste thus ensuring near zero waste to the environment from the crop. The Iron-Zinc incorporation does not alter significantly morphology and particle size of the tablet. In the manufacturing and business sense, the tablet has suitability potential for application in dietary supplement matrix systems. The CWF_I provides good trade-off in terms of the balance between fast disintegration time and mechanical strength of tablet excipients, thus showing potential use in tablets for endusers requiring tablets that release Iron-Zinc easily and fast. For the first time the compatibility of Iron and Zinc in a matrix tablet has been achieved without the need to include extra cost of stabilisers, thus paving way for future possible multiple actives (e.g. combination of more nutrients or nutrients-drug actives in a single matrix) at low-cost. Effective excipient tablet dissolution behaviour allowing full Iron- zinc releases within 30 to 45 min, across all tablet weights, is enhanced by using the preliminary approach of obtaining SRRC-processed safe and inexpensive materials. The recovered waste cassava biomaterial and deployed SRRC in production of starting materials could be a practical and sustainable strategy for scale-up of alternative green production of dietary supplement excipients.

Declaration of Competing Interest

The authors confirm that they have no conflicts of interest with respect to the work described in this manuscript

Acknowledgments

The research fund support provided by National Agricultural Research Organisation (NARO-Uganda) is appreciatively recognised

Supplementary materials

Supplementary material associated with this article can be found, in the online version, at doi:10.1016/j.fufo.2020.100003.

References

Abdel-Shafy, H.I., Mansour, M.S.M., 2018. Solid waste issue: sources, composition, disposal, recycling, and valorization. Egypt. J. Petrol. 27 (4), 1275–1290. doi:10.1016/j.ejpe.2018.07.003.

Abiad, M.G., Meho, L.I., 2018. Food loss and food waste research in the Arab world: a systematic review. Food Secur. 10 (2), 311–322. doi:10.1007/s12571-018-0782-7.

Achor, M., Oyeniyi, J., Musa, M., Gwarzo, M., 2015. Physicochemical properties of cassava starch retrograded in alcohol. J. Appl. Pharm. Sci. 5, 126–131. doi:10.7324/JAPS.2015.501021.

Alexis, S.D., Jean, N.G., 2010. Effect of technological treatments on cassava (Manihot Esculenta Crantz) composition. Food Nutr. Sci. 01 (01), 19–23. doi:10.4236/fns.2010.11004.

Alyami, H., Dahmash, E., Bowen, J., Mohammed, A.R., 2017. An investigation into the effects of excipient particle size, blending techniques and processing parameters on the homogeneity & content uniformity of a blend containing low-dose model drug. PLoS ONE 12 (6), 1–19. doi:10.1371/journal.pone.0178772.

Anderson, C.A.M., Millen, B., 2017. Nutrition guidelines to promote and maintain health. In: Coulston, A.M., Boushey, C.J., Delahanty, L.M. (Eds.), Nutrition in the Prevention and Treatment of Disease. Imp-publishing Acad. Press., USA, p. 239. doi:10.1016/b978-0-12-802928-2.00012-6.

Baker, L., 2015. Mathematical models of drug release. In: Bruschi, M.L (Ed.), Strategies to Modify the Drug Release from Pharmaceutical Systems. Imp-publishing Acad. Press., USA, pp. 63–86. doi:10.1016/b978-0-08-100092-2.00005-9.

Caccavo, D., Cascone, S., Lamberti, G., Barba, A.A., 2015. Modeling the drug release from hydrogel-based matrices. Molec. Pharm. 12 (2), 474–483. doi:10.1021/mp500563n.

Cao, X., Zhang, M., Mujumdar, A.S., Zhong, Q., Wang, Z., 2018. Effect of nano-scale powder processing on physicochemical and nutritional properties of barley grass. Powder Technol. 336, 161–167. doi:10.1016/j.powtec.2018.05.054.

Carr, R.L., 1965. Evaluating flow properties of solids. Chem. Eng. J. 72, 163–168.

Censi, R., Di Martino, P., 2015. Polymorph impact on the bioavailability and stability of poorly soluble drugs. Molecules 20 (10), 18759–18776. doi:10.3390/molecules201018759.

Chattoraj, S., Daugherity, P., McDermott, T., Olsofsky, A., Roth, W.J., Tobyn, M., 2018. Sticking and picking in pharmaceutical tablet compression: an IQ consortium review. J. Pharm. Sci. 107 (9), 2267–2282. doi:10.1016/j.xphs.2018.04.029.

Chatzizaharia, K.A., Hatziavramidis, D.T., 2015. Dissolution efficiency and design space for an oral pharmaceutical product in tablet form. Ind. Eng. Chem. Res. 54 (24), 6305–6310. doi:10.1021/ie5050567.

Chen, Q.M., Fu, M.R., Yue, F.L., Cheng, Y.Y., 2015. Effect of superfine grinding on physicochemical properties, antioxidant activity and phenolic content of red rice (*Oryza sativa* L.). Food Nutr. Sci. 06 (14), 1277–1284. doi:10.4236/fns.2015.614133.

Choi, Y., Andrade Korn, M. das G., da Boa Morte, E.S., Batista dos Santos, D.C.M., Castro, J.T., Barbosa, J.T.P., Teixeira, A.P., Fernandes, A.P., Welz, B., dos Santos, W.P C., Nunes dos Santos, E.B G., Korn, M., Epa, U.S., FAO, WHO, CODEX, 1995, Paranagama, P., Elledge, M.F., Redmon, J.H., … Lanka, S. (2011). FAO/WHO. 14(2), 1–48. 10.3768/rtipress.2014.rb.0007.1405

Dangre, P.V., Godbole, M.D., Ingale, P.V., Mahapatra, D.K., 2016. Improved dissolution and bioavailability of eprosartan mesylate formulated as solid dispersions using conventional methods. Indian J. Pharm. Educ. Res. 50 (3), S209–S217. doi:10.5530/ijper.50.3.31.

Daud, Z., Kassim, M., Sari, A., MohdAripin, A., Awang, H., Hatta, M., Zainuri, M., 2013. Chemical composition and morphological of cocoa pod husks and cassava peels for pulp and paper production. Aust. J. Basic Appl. Sci. 7, 406–411.

De Araújo, F.D.C.B., Moura, E.F., Cunha, R.L., De Farias Neto, J.T., De Souza Silva, R., 2019. Chemical root traits differentiate 'bitter' and 'sweet' cassava accessions from the Amazon. Crop Breed. Appl. Biotechnol. 19 (1), 77–85. doi:10.1590/1984-70332019v19n1a11.

Diaz, D.A., Colgan, S.T., Langer, C.S., Bandi, N.T., Likar, M.D., Van Alstine, L., 2016. Dissolution similarity requirements: how similar or dissimilar are the global regulatory expectations? AAPS J. 18 (1), 15–22. doi:10.1208/s12248-015-9830-9.

Dietary Reference Values for nutrients Summary report. 2017. EFSA Supporting Publications 14(12). 10.2903/sp.efsa.2017.e15121

Donangelo, C.M., Woodhouse, L.R., King, S.M., Viteri, F.E., King, J.C., 2002. Supplemental zinc lowers measures of iron status in young women with low iron reserves. J. Nutr. 132 (7), 1860–1864. doi:10.1093/jn/132.7.1860.

Dürig, T., Venkatesh, G.M., Fassihi, R., 1999. An investigation into the erosion behaviour of a high drug-load (85%) particulate system designed for an extended-release matrix tablet. Analysis of erosion kinetics in conjunction with variations in lubrication, porosity and compaction rate. J. Pharm. Pharmacol. 51 (10), 1085–1092. doi:10.1211/0022357991776769.

Efentakis, M., Buckton, G., 2002. The effect of erosion and swelling on the dissolution of theophylline from low and high viscosity sodium alginate matrices. Pharm. Dev. Technol. 7 (1), 69–77. doi:10.1081/PDT-120002232.

E Silva, J.P.S., Splendor, D., Gonçalves, I.M.B., Costa, P., Sousa Lobo, J.M., 2013. Note on the measurement of bulk density and tapped density of powders according to the European pharmacopeia. AAPS PharmSciTech 14 (3), 1098–1100. doi:10.1208/s12249-013-9994-5.

European, T.H.E., The, D.F.O.R., Medicines, Q.O.F., 2019. *The European directorate for the quality of medicines enabling QbD and Continuous. September*.

Eyjolfsson, R.,. 2014. Design and manufacture of pharmaceutical tablets. 10.1016/C2014-0-02382-9

Fan Liang-tseng, S.S.K., 1989. Diffusion-Controlled Release. Springer, Berlin, Heidelberg doi:10.1007/978-3-642-74507-2.

FAO. 2020. Food agricultural organisation. Save food global food waste and loss initiative. http://www.fao.org/save-food/resources/keyfindings/en/

FAO. 2015. Food agricultural organisation. The state of food insecurity in the world. http://www.fao.org/hunger/key-messages/en/

FAO. 2013. Food wastage footprint: impacts on natural resources. Summary Report. pp.61. http://www.fao.org/3/i3347e/i3347e.pdf

Firth, J., Teasdale, S.B., Allott, K., Siskind, D., Marx, W., Cotter, J., Veronese, N., Schuch, F., Smith, L., Solmi, M., Carvalho, A.F., Vancampfort, D., Berk, M., Stubbs, B., Sarris, J., 2019. The efficacy and safety of nutrient supplements in the treatment of mental disorders: a meta-review of meta-analyses of randomized controlled trials. World Psychol. 18 (3), 308–324. doi:10.1002/wps.20672.

Food and Drug Administration, 2019. Bioavailability studies submitted in NDAs or INDs – General considerations. Draft Guidance.

Fritsch, C., Staebler, A., Happel, A., Márquez, M.A.C., Aguiló-Aguayo, I., Abadias, M., Gallur, M., Cigognini, I.M., Montanari, A., López, M.J., Suárez-Estrella, F., Brunton, N., Luengo, E., Sisti, L., Ferri, M., Belotti, G., 2017. Processing, valorization and application of bio-waste derived compounds from potato, tomato, olive and cereals: a review. Sustainability 9 (8), 1–46. doi:10.3390/su9081492.

Gabbott, I.P., Al Husban, F., Reynolds, G.K., 2016. The combined effect of wet granulation process parameters and dried granule moisture content on tablet quality attributes. Eur. J. Pharm. Biopharm. 106, 70–78. doi:10.1016/j.ejpb.2016.03.022.

Galanakis, C.M., 2013. Emerging technologies for the production of nutraceuticals from agricultural byproducts: a viewpoint of opportunities and challenges. Food Bioprod. Proc. 91 (4), 575–579. doi:10.1016/j.fbp.2013.01.004.

Galanakis, C.M., 2020. The food systems in the era of the Coronavirus (COVID-19) pandemic crisis. Food 2 (4), 523. doi:10.3390/foods9040523.

Gibaldi, M., Feldman, S., 1967. Establishment of sink conditions in dissolution rate determinations. Theoretical considerations and application to nondisintegrating dosage forms. J. Pharm. Sci. 56 (10), 1238–1242. doi:10.1002/jps.2600561005.

Glaessl, B., Siepmann, F., Tucker, I., Rades, T., Siepmann, J., 2010. Mathematical modeling of drug release from Eudragit RS-based delivery systems. J. Drug Deliv. Sci. Technol. 20 (2), 127–133. doi:10.1016/S1773-2247(10)50017-0.

Grdešič, P., Vrečer, F., Ilić, I., 2016. Flow and compaction properties of hypromellose: new directly compressible versus the established grades. Drug Dev. Ind. Pharm. 42 (11), 1877–1886. doi:10.1080/03639045.2016.1181079.

Green, G., Berg, C., Polli, J.E., Dirk, M., 2015. Pharmacopeial standards for the subdivision characteristics of scored tablets pharmacopeial standards for the subdivision characteristics of scored tablets. Pharm. Forum 35 (6), 1598–1612. doi:10.13140/2.1.4057.6807, (December 2009).

Hausner, H.H., 1981. Powder characteristics and their effect on Powder processing. Powder Technol. 30 (1), 3–8. doi:10.1016/0032-5910(81)85021-8.

He, S., Li, J., He, Q., Jian, H., Zhang, Y., Wang, J., Sun, H., 2018. Physicochemical and antioxidant properties of hard white winter wheat (*Triticum aestivm* L.) bran superfine powder produced by eccentric vibratory milling. Powder Technol. 325, 126–133. doi:10.1016/j.powtec.2017.10.054.

Hindi, S., Hindi, S.S.Z., 2016. Microcrystalline cellulose: its processing and pharmaceutical specifications. BioCryl. J. 1 (1), 26–38.

Hsu, T.T., Langer, R., 1985. Polymers for the controlled release of macromolecules: effect of molecular weight of ethylene-vinyl acetate copolymer. J. Biomed. Mater. Res. 19 (4), 445–460. doi:10.1002/jbm.820190409.

Ishangulyyev, R., Kim, S., Lee, S.H., 2019. Understanding food loss and waste-why are we losing and wasting food? Foods 8 (8), 1–23. doi:10.3390/foods8080297.

Jan, S., Ambrose, R.P.K., Saxena, D.C., 2017. Effect of grinding action on the flowability of rice flour. J. Food Meas. Charact. 11 (2), 801–811. doi:10.1007/s11694-016-9451-8.

Juban, A., Nouguier-Lehon, C., Briancon, S., Hoc, T., Puel, F., 2015. Predictive model for tensile strength of pharmaceutical tablets based on local hardness measurements. Int. J. Pharm. 490 (1–2), 438–445. doi:10.1016/j.ijpharm.2015.05.078.

Kapoor, D., Maheshwari, R., Verma, K., Sharma, S., Pethe, A., Tekade, R.K., 2020. Fundamentals of diffusion and dissolution: dissolution testing of pharmaceuticals. Drug Deliv. Syst. 1–45. doi:10.1016/B978-0-12-814487-9.00001-6.

Kaptoge, S., Pennells, L., De Bacquer, D., Cooney, M.T., Kavousi, M., Stevens, G., Riley, L.M., Savin, S., Khan, T., Altay, S., Amouyel, P., Assmann, G., Bell, S., Ben-Shlomo, Y., Berkman, L., Beulens, J.W., Björkelund, C., Blaha, M., Blazer, D.G., … Di Angelantonio, E., 2019. World health organization cardiovascular disease risk charts: revised models to estimate risk in 21 global regions. Lancet Glob. Health 7 (10), e1332–e1345. doi:10.1016/S2214-109X(19)30318-3.

Katzhendler, I., Hoffman, A., Goldberger, A., Friedman, M., 1997. Modeling of drug release from erodible tablets. J. Pharm. Sci. 86 (1), 110–115. doi:10.1021/js9600538.

Kemausuor, F., Addo, A., Darkwah, L., 2015. Technical and socioeconomic potential of biogas from cassava waste in Ghana. Biotechnol. Res. Int. 2015, 1–10. doi:10.1155/2015/828576.

Khadka, P., Ro, J., Kim, H., Kim, I., Kim, J.T., Kim, H., Cho, J.M., Yun, G., Lee, J., 2014. Pharmaceutical particle technologies: an approach to improve drug solubility, dissolution and bioavailability. Asian J. Pharm. Sci. 9 (6), 304–316. doi:10.1016/j.ajps.2014.05.005.

Khan, K.A., 1975. The concept of dissolution efficiency. J. Pharm. Pharmacol. 27 (1), 48–49. doi:10.1111/j.2042-7158.1975.tb09378.x.

Kumar, A., Nanda, A., 2018. Design and optimization of ezetimibe self microemulsifying drug delivery system for enhanced therapeutic potential. Drug Deliv. Lett. 08. doi:10.2174/2210303108666180528074708.

Lamoudi, L., Chaumeil, J.C., Daoud, K., 2016. Swelling, erosion and drug release characteristics of sodium diclofenac from heterogeneous matrix tablets. J. Drug Deliv. Sci. Technol. 31, 93–100. doi:10.1016/j.jddst.2015.12.005.

Leite, A.L.M.P., Zanon, C.D., Menegalli, F.C., 2017. Isolation and characterisation of cellulose nanofibres from cassava root bagasse and peelings. Carbohydr. Polym. 157, 962–970. doi:10.1016/carbpol.2016.10.048.

Li, J., Mooney, D.J., 2016. Designing hydrogels for controlled drug delivery. Nat. Rev. Mater. 1 (12), 1–17. doi:10.1038/natrevmats.2016.71.

Lin, C.S.K., Pfaltzgraff, L.A., Herrero-Davila, L., Mubofu, E.B., Abderrahim, S., Clark, J.H., Koutinas, A.A., Kopsahelis, N., Stamatelatou, K., Dickson, F., Thankappan, S., Mohamed, Z., Brocklesby, R., Luque, R., 2013. Food waste as a valuable resource for the production of chemicals, materials and fuels. Current situation and global perspective. Energy Environ. Sci. 6 (2), 426–464. doi:10.1039/c2ee23440h.

Maghsoodi, M., Yari, Z., 2015. Effect of drying phase on the agglomerates prepared by spherical crystallization. Iran. J. Pharm. Res. 14 (1), 51–57. doi:10.22037/ijpr.2015.1628.

Malucelli, L.C., Lacerda, L.G., Dziedzic, M., da Silva Carvalho Filho, M.A., 2017. Preparation, properties and future perspectives of nanocrystals from agro-industrial residues: a review of recent research. Rev. Environ. Sci. Bio/Technol. 16 (1), 131–145. doi:10.1007/s11157-017-9423-4.

Manalo, R.A.M., Arollado, E.C., Pellazar, J.M.M., Siocson, M.P.F., Ramirez, R.L.F., 2018. Yellow Mangifera indica Linn. And Artocarpus heterophyllus Lam. Seed starch as binder and disintegrant in paracetamol tablet formulation. J. Appl. Pharm. Sci. 8 (3), 60–66. doi:10.7324/JAPS.2018.8309.

Manano, J., Ogwok, P., Byarugaba-Bazirake, G.W., 2017. Chemical composition of major cassava varieties in Uganda, targeted for industrialisation. J. Food Res. 7 (1), 1. doi:10.5539/jfr.v7n1p1.

Markl, D., Zeitler, J.A., 2017. A review of disintegration mechanisms and measurement techniques. Pharm. Res. 34 (5), 890–917. doi:10.1007/s11095-017-2129-z.

Martínez-Ballesta, M.C., Gil-Izquierdo, Á., García-Viguera, C., Domínguez-Perles, R., 2018. Nanoparticles and controlled delivery for bioactive compounds: outlining challenges for new "smart-foods" for health. Food 7 (5), 1–29. doi:10.3390/foods7050072.

Martins, J.T., Ramos, Ó.L., Pinheiro, A.C., Bourbon, A.I., Silva, H.D., Rivera, M.C., Cerqueira, M.A., Pastrana, L., Malcata, F.X., González-Fernández, Á., Vicente, A.A., 2015. Edible bio-based nanostructures: delivery, absorption and potential toxicity. Food Eng. Rev. 7 (4), 491–513. doi:10.1007/s12393-015-9116-0.

McConville, J., Ross, A., Florence, A., Stevens, H., 2005. Erosion characteristics of an erodible tablet incorporated in a time-delayed capsule device. Drug Dev. Ind. Pharm. 31 (1), 79–89. doi:10.1081/ddc-200044010.

McKey, D., Cavagnaro, T.R., Cliff, J., Gleadow, R., 2010. Chemical ecology in coupled human and natural systems: people, manioc, multitrophic interactions and global change. Chemoecology 20 (2), 109–133. doi:10.1007/s00049-010-0047-1.

Mhase, S.R., Nanjwade, B.K., Sarkar, A.B., Srichana, T., 2018. Development and evaluation of dual release tablet of metformin and pioglitazone for the treatment of diabetes mellitus. Pharm. Anal. Acta 09 (04). doi:10.4172/2153-2435.1000583.

Morovati, A., Ghaffari, A., Jabarian, L.E., Mehramizi, A., 2017. Single layer extended release two-in-one guaifenesin matrix tablet: formulation method, optimization, release kinetics evaluation and its comparison with mucinex® using box-behnken design. Iran. J. Pharm. Res. 16 (4), 1349–1369. doi:10.22037/ijpr.2017.2144.

Moss, J.W.E., Williams, J.O., Ramji, D.P., 2018. Nutraceuticals as therapeutic agents for atherosclerosis. Biochim. Biophys. Acta Mol. Basis Dis. 1864 (5), 1562–1572. doi:10.1016/j.bbadis.2018.02.006.

Murugesan, R., Orsat, V., 2012. Spray drying for the production of nutraceutical ingredients—A review. Food Bioprocess Technol. 5, 3–14. doi:10.1007/s11947-011-0638-z.

Mushumbusi, C.B., Max, R.A., Bakari, G.G., Mushi, J.R., Balthazary, S.T., 2020. Cyanide in cassava varieties and people's perception on cyanide poisoning in selected regions of Tanzania. J. Agric. Stud. 8 (1), 180. doi:10.5296/jas.v8i1.15511.

Mužíková, J., Komersová, A., Lochař, V., Vildová, L., Vošoustová, B., Bartoš, M., 2018. Comparative evaluation of the use of dry binders in a physical mixture or as a coprocessed dry binder in matrix tablets with extended drug release. Acta Pharm. 68 (3), 295–311. doi:10.2478/acph-2018-0030.

Nep, E.I., Asare-Addo, K., Ghori, M.U., Conway, B.R., Smith, A.M., 2015. Starch-free grewia gum matrices: compaction, swelling, erosion and drug release behaviour. Int. J. Pharm. 496 (2), 689–698. doi:10.1016/j.ijpharm.2015.10.071.

Ngwuluka, N.C., Idiakhoa, B.A., Nep, E.I., Ogaji, I., Okafor, I.S., 2010. Formulation and evaluation of paracetamol tablets manufactured using the dried fruit of Phoenix dactylifera Linn as an excipient. Res. Pharm. Biotechnol. 2 (3), 25–32. http://www.academicjournals.org/RPB.

Nirmala, R., Suresh, G., 2018. Development and in vivo evaluation of nelfinavir extended release trilayer matrix tablets in the management of AIDS. Int. J. Pharm. Sci. Drug Res. 10 (4), 342–350. doi:10.25004/ijpsdr.2018.100421.

Njankouo Ndam, Y., Mounjouenpou, P., Kansci, G., Kenfack, M.J., Fotso Meguia, M.P., Natacha Ngono Eyenga, N.S., Mikhaïl Akhobakoh, M., Nyegue, A., 2019. Influence of cultivars and processing methods on the cyanide contents of cassava (Manihot esculenta Crantz) and its traditional food products. Sci. Afr. 5, e0019. doi:10.1016/j.sciaf.2019.e00119, 1-8.

Nokhodchi, A., 2005. Effect of Moisture on compaction and compression. Pharm. Technol. 29, 46–66.

Oketch-rabah, H.A., Hardy, M.L., Patton, A.P., Chung, M., Sarma, N.D., Yoe, C., Ayyadurai, V.A.S., Fox, M.A., Jordan, S.A., Mwamburi, M., Mould, D.R., Osterberg, R.E., Hilmas, C., Tiwari, R., Jr, L.V., Jones, D., Patricia, A., Giancaspro, G.I., Hardy, M.L., … Decision, G.I.G.M., 2020. Multi-criteria decision analysis model for assessing the risk from multi-ingredient dietary supplements (MIDS). J. Diet. Suppl. 0 (0), 1–23. doi:10.1080/19390211.2020.1741485.

Osamura, T., Takeuchi, Y., Onodera, R., Kitamura, M., Takahashi, Y., Tahara, K., Takeuchi, H., 2017. Prediction of effects of punch shapes on tableting failure by using a multi-functional single-punch tablet press. Asian J. Pharm. Sci. 12 (5), 412–417. doi:10.1016/j.ajps.2017.05.001.

Patel, V., Patel, S., 2013. Delivering drug-polymer complex via quick dissolving film: a step towards the development of an appropriate pediatric formulation. Asian J. Pharm. 7 (1), 21–26. doi:10.4103/0973-8398.110932.

Peppas, N.A., Duncan, R., Wnek, G.E., Hoffman, A..., Gao, G.H., Kim, S.W., Lee, D.S., Hadjiargyrou, M., Touitou, E., Ainbinder, D., Mumper, R., Rolland, A., Niidome, T., Labhasetwar, V., Liu, S., Zhou, G., Huang, Y., Xie, Z., Jing, X., … Mitragotri, S., 2014. Highly cited research articles in Journal of Controlled Release: commentaries and perspectives by authors. J. Control. Rel. 190, 29–74. doi:10.1016/S0168-3659(14)00482-9.

Phillips, D.J., Pygall, S.R., Brett Cooper, V., Mann, J.C., 2012. Toward biorelevant dissolution: application of a biphasic dissolution model as a discriminating tool for HPMC matrices containing a model BCS class II drug. Diss. Technol. 19 (1), 25–34. doi:10.14227/DT190112P25.

Psimadas, D., Georgoulias, P., Valotassiou, V., Loudos, G., 2012. Molecular nanomedicine towards cancer. J. Pharm. Sci. 101 (7), 2271–2280. doi:10.1002/jps.

Raghavendra, S.N., Rastogi, N.K., Raghavarao, K.S.M.S., Tharanathan, R.N., 2004. Dietary fiber from coconut residue: effects of different treatments and particle size on the hydration properties. Eur. Food Res. Technol. 218 (6), 563–567. doi:10.1007/s00217-004-0889-2.

Ritger, P.L., Peppas, N.A., 1987. A simple equation for description of solute release II. Fickian and anomalous release from swellable devices. J. Control. Rel. 5 (1), 37–42. doi:10.1016/0168-3659(87)90035-6.

Roohani, N., Hurrell, R., Kelishadi, R., Schulin, R., 2013. Zinc and its importance for human health: an integrative review. J. Res. Med. Sci. 18 (2), 144–157. https://pubmed.ncbi.nlm.nih.gov/23914218.

Saccone, C.D., Tessore, J., Olivera, S.A., Meneces, N.S., 2004. Statistical properties of the dissolution test of USP. Diss. Technol. 11 (3), 25–28. doi:10.14227/DT110304P25.

SahabUddin, M., Al Mamun, A., Tasnu, T., Asaduzzaman, M., 2015. In-process and finished products quality control tests for pharmaceutical tablets according to pharmacopoeias. J. Chem. Pharm. Res. 7 (9), 180–185.

Saifullah, M., Yusof, Y.A., Chin, N.L., Aziz, M.G., Mohammed, M.A.P., Aziz, N.A., 2014. Tableting and dissolution characteristics of mixed fruit powder. Agric. Agric. Sci. Proc. 2, 18–25. doi:10.1016/j.aaspro.2014.11.004.

Schmid, K., Löbenberg, R., 2010. Influence of the changed USP specifications on disintegration test performance. Diss. Technol. 17 (1), 6–10. doi:10.14227/DT170110P6.

Schrenk, D., Bignami, M., Bodin, L., Chipman, J.K., del Mazo, J., Grasl-Kraupp, B., Hogstrand, C., Hoogenboom, L., Leblanc, J.C., Nebbia, C.S., Nielsen, E., Ntzani, E., Petersen, A., Sand, S., Vleminckx, C., Wallace, H., Benford, D., Brimer, L., Mancini, F.R., … Schwerdtle, T., 2019. Evaluation of the health risks related to the presence of cyanogenic glycosides in foods other than raw apricot kernels. EFSA J. 17 (4), 5662. doi:10.2903/j.efsa.2019.5662, 1-78.

Shah, R.B., Tawakkul, M.A., Khan, M.A., 2008. Comparative evaluation of flow for pharmaceutical powders and granules. AAPS Pharm. Sci. Technol. 9 (1), 250–258. doi:10.1208/s12249-008-9046-8.

Sharma, N., Pahuja, S., Sharma, N., 2019. Immediate release tablets: a review. Int. J. Pharm. Sci. Res. 10 (8), 3607–3618 10.13040/IJPSR.0975-8232.10(8).3607-18.

Sharp, P., Srai, S.K., 2007. Molecular mechanisms involved in intestinal iron absorption. Sharp P, Srai SK. Author information. 13(2), 17729393.

Shoaib, M.H., Al Sabah Siddiqi, S., Yousuf, R.I., Zaheer, K., Hanif, M., Rehana, S., Jabeen, S., 2010. Development and evaluation of hydrophilic colloid matrix of famotidine tablets. AAPS Pharm. Sci. Technol. 11 (2), 708–718. doi:10.1208/s12249-010-9427-7.

Siepmann, J., Peppas, N.A., 2012. Modeling of drug release from delivery systems based on hydroxypropyl methylcellulose (HPMC). Adv. Drug Del. Rev. 64 (SUPPL.), 163–174. doi:10.1016/j.addr.2012.09.028.

Silva, J.D.O., Santos, D.E.L., Abud, A.K., de, S., de Oliveira, M., 2020. Characterization of acerola (Malpighia emarginata) industrial waste as raw material for thermochemical processes. Waste Manag. 107, 143–149. doi:10.1016/j.wasman.2020.03.037.

Stevens, R.E., Gray, V., Dorantes, A., Gold, L., Pham, L., 2015. Scientific and regulatory standards for assessing product performance using the similarity factor, f2. AAPS J. 17 (2), 301–306. doi:10.1208/s12248-015-9723-y.

Suleria, H.A.R., Osborne, S., Masci, P., Gobe, G., 2015. Marine-based nutraceuticals: an innovative trend in the food and supplement industries. Mar. Drug 13 (10), 6336–6351. doi:10.3390/md13106336.

Sun, C., 2005. True density of microcrystalline cellulose. J. Pharm. Sci. 94 (10), 2132–2134. doi:10.1002/jps.20459.

Thoorens, G., Krier, F., Leclercq, B., Carlin, B., Evrard, B., 2014. Microcrystalline cellulose, a direct compression binder in a quality by design environment - A review. Int. J. Pharm. 473 (1–2), 64–72. doi:10.1016/j.ijpharm.2014.06.055.

Tian, J., Liu, E., Jiang, L., Jiang, X., Sun, Y., Xu, R., 2018. Influence of particle shape on the microstructure evolution and the mechanical properties of granular materials. C. R. Mec 346 (6), 460–476. doi:10.1016/j.crme.2018.03.006.

Torres-León, C., Ramírez-Guzman, N., Londoño-Hernandez, L., Martinez-Medina, G.A., Díaz-Herrera, R., Navarro-Macias, V., Alvarez-Pérez, O.B., Picazo, B., Villarreal-Vázquez, M., Ascacio-Valdes, J., Aguilar, C.N., 2018. Food waste and byproducts: an opportunity to minimize malnutrition and hunger in developing countries. Front. Sustain. Food Syst. 2 (52), 1–17. doi:10.3389/fsufs.2018.00052.

Tumwesigye, K.S., Oliveira, J.C., Sousa-Gallagher, M.J., 2016a. New sustainable approach to reduce cassava borne environmental waste and develop biodegradable materials for food packaging applications. Food Pack. Shelf. 7, 8–19. doi:10.1016/j.fpsl.2015.12.001.

Tumwesigye, K.S., Morales-Oyervides, L., Oliveira, J.C., Sousa-Gallagher, M.J., 2016b. Effective utilisation of cassava bio-wastes through integrated process design: a sustainable approach to indirect waste management. Proc. Saf. Env. Prot. 102, 159–167. doi:10.1016/j.psep.2016.03.008.

Tumwesigye, K.S., Peddapatla, R.V.G., Crean, A., Oliveira, J.C., Sousa-Gallagher, M.J., 2016c. Integrated process standardisation as zero-based approach to bitter cassava waste elimination and widely-applicable industrial biomaterial derivatives. Chem. Eng. Proc. Proc. Intens. 108, 139–150. doi:10.1016/j.cep.2016.08.004.

Tumwesigye, K.S., Sousa, A.R., Oliveira, J.C., Sousa-Gallagher, M.J., 2017. Evaluation of novel bitter cassava film for equilibrium modified atmosphere packaging of cherry tomatoes. Food Pack. Shelf. 13, 1–14. doi:10.1016/j.fpsl.2017.04.007.

Varzakas, T., Zakynthinos, G., Verpoort, F., 2016. Plant food residues as a source of nutraceuticals and functional foods. Food 5 (4), 88. doi:10.3390/foods5040088.

Versino, F., López, O.V., García, M.A., 2015. Sustainable use of cassava (Manihot esculenta) roots as raw material for biocomposites development. Ind. Crop Prod. 65, 79–89. doi:10.1016/j.indcrop.2014.11.054.

Vodáčková, P., Vraníková, B., Svačinová, P., Franc, A., Elbl, J., Muselík, J., Kubalák, R., Solný, T., 2018. Evaluation and comparison of three types of spray dried coprocessed excipient avicel® for direct compression. Biomed. Res. Int. doi:10.1155/2018/2739428, 2018.

Wade, J.B., Martin, G.P., Long, D.F., 2013. A methodological approach for determining the effect of moisture content on the compaction properties of powders: granular hydroxyapatite. Powder Technol. 246, 511–519. doi:10.1016/j.powtec.2013.06.017.

Wagner, J.G., 1969. Interpretation of percent dissolved-time plots derived from in vitro testing of conventional tablets and capsules. J. Pharm. Sci. 58 (10), 1253–1257. doi:10.1002/jps.2600581021.

Widiarto, S., Pramono, E., Suharso, Rochliadi, A., Arcana, I.M., 2019. Cellulose nanofibers preparation from cassava peels via mechanical disruption. Fiber 7, 44. doi:10.3390/fib7050044.

World Health Organization, 2011. Revision of monograph on tablets. Final text for addition. Int. Pharm. 1–6. March http://www.who.int/medicines/publications/pharmacopoeia/Tabs-GeneralMono-rev-FINAL_31032011.pdf .

World Health Organisation, 2019. Index of world pharmacopoeias and pharmacopoeial authorities. Working document QAS/11.453/Rev.11. pp. 1–52.

World Health Organisation, 2020. Dissolution test for solid oral dosage forms, draft proposal for revision in the international pharmacopoeia. https://www.who.int/medicines/areas/quality_safety/quality_assurance/QAS20_837_Dissolution_Test_For_Solid_Oral_Dosage_Forms.pdf?ua=1

Xi, H., Dou, J., Li, D., Wang, L., 2018. Effects of superfine grinding on properties of sugar beet pulp powders. LWT Food Sci. Technol. 87, 203–209. doi:10.1016/j.lwt.2017.08.067.

Zhang, X., Xing, H., Zhao, Y., Ma, Z., 2018. Pharmaceutical dispersion techniques for dissolution and bioavailability enhancement of poorly water-soluble drugs. Pharmaceutics 10 (3). doi:10.3390/pharmaceutics10030074.

Zhao, X., Zhu, H., Zhang, G., Tang, W., 2015. Effect of superfine grinding on the physicochemical properties and antioxidant activity of red grape pomace powders. Powder Technol. 286, 838–844. doi:10.1016/j.powtec.2015.09.025.

Zhu, F.M., Du, B., Li, J., 2014. Effect of ultrafine grinding on physicochemical and antioxidant properties of dietary fiber from wine grape pomace. Food Sci. Technol. Int. 20 (1), 55–62. doi:10.1177/1082013212469619.